SCIENCE OF LIGHT

VOLUME 5 NUMBER 2

September
1956

Published by the

Institute for Optical Research

Tokyo University of Education

in collaboration with the

The Spectroscopical Society of Japan

SCIENCE OF LIGHT

Science of Light contains reports of the Institute for Optical Research and contributions from other science bodies about similar subjects.

All communications should be addressed to the director or to the librarian of the Institute.

The Institute for Optical Research

Tokyo University of Education

400, 4-chome, Hyakunin-machi, Sinjuku-ku, Tokyo, Japan

Printed at
Kokusai Bunken Insatsusha
Chiyoda-ku, Tokyo.

An Investigation of the Properties of Bolometers made by Vacuum Evaporation

Kunio YOSIHARA

Department of Applied Physics, Faculty of Engineering, Nagoya University

(Received May 17, 1956)

Abstract

Although the signal-to-noise ratio is independent of the bolometer resistance, the output voltage of a bolometer increases with its electrical resistance. This means a great simplification of the amplifying system when a bolometer is made of a substance with high resistance. The high resistance bolometer, however, must be prepared by vacuum evaporation, hence the falling off of the temperature coefficient of resistance as well as the current noise presents a serious problem in improving its performance.

In the present experiment, bismuth and tellurium are used to make evaporated bolometers. The variation of temperature coefficient with film thickness is first determined, and at the same time the dependence of the amount of current noise on the thickness of the bolometer strip and the substrate or on other factors is carefully examined to find the best conditions. Thus it is found that tellurium is not suitable for the evaporated bolometer on account of its appreciable current noise, but excellent bolometers can be made of bismuth provided both the strip and the substrate are sufficiently thick.

Also the sensitization of the evaporated film with gold in amount equivalent to a few tenth of a monolayer improved the performance of the bolometer remarbably.

A typical bolometer of bismuth possesses a resistance of about 1000 ohms, and its sensitivity is between 20 and 30 μw/μv when the current of 2 milliamperes is passed through it. The time constant determined from the frequency characteristics lies between 60 and 90 milliseconds.

The bolometer is used as a detector of an infra-red spectrometer equipped with a lithium fluoride prism, and several infra-red spectra are recorded on photographic papers by a simple self-recording device. From the examination of these spectra, it is concluded that a bolometer with high electrical resistance prepared by vacuum evaporation works as successfully as any other infra-red detector.

1. Introduction

According to the thory of bolometers[1], the electromotive force δe generated by a periodical radiation $\delta P \cos \omega t$ falling on the bolometer is

1) B. H. Billings, W. L. Hyde and E. F. Barr: J.O.S.A. **37** (1947) 123.

$$\delta e=\left(\frac{\beta\varphi}{h^2\omega^2+\beta^2}\right)^{1/2}\alpha\sqrt{R}\,\delta P \qquad (1)$$

where R is the resistance of the bolometer, α its temperature coefficient, β its cooling constant, φ the highest temperature at which it can be operated, and h its heat capacity. Provided that the minimum detectable power is limited only by the Johnson noise, the signal to noise ratio S is

$$S=\frac{\alpha}{2(kT\Delta f)^{1/2}}\left(\frac{\beta\varphi}{h^2\omega^2+\beta^2}\right)^{1/2} \qquad (2)$$

where Δf is the band pass of the measuring system, k the Boltzmann constant and T the absolute temperature. Apparently this ratio is independent of the bolometer resistance and proportional to the temperature coefficient. Accordingly, other things being equal, it is clearly desirable to use a material with large temperature coefficient of electrical resistance, which is also expected by elementary considerations. On the other hand, by the formula (1) the electromotive force caused by the radiation is proportional to the square root of the electrical resistance. This situation suggests that the amplifying system can be greatly simplified and furthermore the external noise becomes less troublesome if a bolometer of high resistance is employed. For these reasons, bolometers made of bismuth, tellurium or other substances with high electrical resistance are counted upon as more convenient than the ordinary metal bolometers. As these materials are too brittle to be rolled into thin foils, the bolometers must be prepared by vacuum evaporation. The bolometers made by evaporation, however, possess the following undesirable characteristics:

1) Their temperature coefficients of electrical resistance are generally smaller than the bulk values.

2) In some cases a large amount of current noise occurs which makes the measurement of small intensity of radiation quite impossible.

Unless these defects are eliminated, good bolometers suitable for the measurement of radiation cannot be constructed. According to the author's preliminary experiment, the temperature coefficient of evaporated films and the amount of current noise depend not only on the properties of evaporated materials and the film thickness, but also on the nature and thickness of the substrates and the method of their preparation. Therefore, the investigations were carried out to make clear the influences of these factors on the characteristics of the bolometer and to improve its performance as a radiation detector.

2. Construction of the Bolometer

As shown in Fig. 1, a hole of the proper size is made in the center of a plate of synthetic resign and across the hole two screws, which are to serve as electrodes, are forced through the plate by heating them and pressed flat to make their heads sunken flush with the surface which is then ground with carborundun as flat as possible. Collodion membrane is affixed on the surface leaving the screw heads clean by wiping them with a wad of cotton wool wetted with amyl-acetate and then by scraping with a razor blade. The metal which is to form the bolometer strip of $0.15\times 8\,mm^2$ is evaporated in a high vacuum onto the collodion membrane screened by a templet. Then the strip is blackened with bismuth black. It is advisable to evaporate a conductive metal heavily on and near the electrodes to secure good electrical contacts.

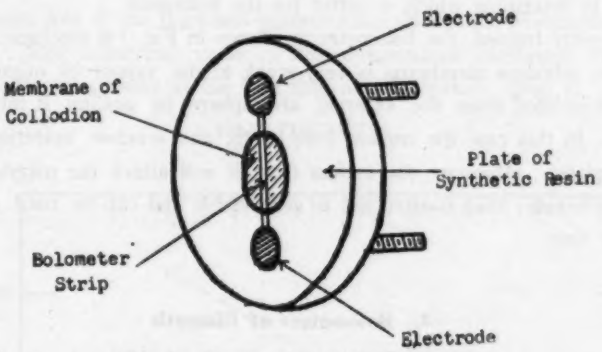

Fig. 1. Construction of the Bolometer

Two methods were used to prepare the membrane of collodion.

The first method: This is essentially the method due to Czerny[2]. The membrane is made by dropping a solution of collodion in amylacetate onto the surface of dust free water in a bowl and soon after the solvent has evaporated away, the membrane is taken out with a suitable frame. By this method a very thin membrane can be obtained.

The second method: This method was employed formerly by Sakurai and others at Tohoku University in order to made thermocouples by evaporation. A solution of collodion in ethyl-ether is spread on a plate of glass and a frame which is to support the membrane is pressed on it before the membrame becomes perfectly dry. Then with a pair of tweezers the membrane is stripped

2) M. Czerny und P. M. Mollet: Z. Physik **108** (1938) 85.

off carefully from the glass surface so that it remains stuck to the frame without crumples. The membrane thus prepared is stretched tight by its own tension and proved to be very strong. It is, however, difficult to obtain very thin membranes by this method. They are much thicker than those made by Czerny's method. Besides, as will be decribed in later sections, the metal film evaporated on this membrane does not possess stable physical properties, and as a result of this, a fairly large amount of current noise is generated when electric current is passed through it. Hence, the membrane of collodion was made chiefly by the first method in the present experiments.

By placing a block of metal of large heat capacity close to the back of the membrane during evaporation, it is possible to prevent the membrane from being heated up to some extent. Properties of the film thus obtained are in some cases fairly different from those of the film evaporated without cooling, and it is not so simple to determine which is better for the bolometer.

If properly treated, the bolometer as shown in Fig. 1 is mechanically strong, but, as the collodion membrane is very weak to the vapour of organic solvent, it must be isolated from the external atmosphere by sealing it into a suitable enclosure. In this case the cement used to fix the window material should be dried completely, otherwise the vapour from it will attack the membrane.

The bolometer thus constructed is very stable and can be used successfully for a long time.

3. Bolometers of Bismuth

(1) Bolometer strip on the membrane of collodion made by the first method

(A) Temperature coefficient of electrical resistance.

During evaporation the membrane was cooled by a block of metal set close to its back. As is known, the evaporated film of bismuth shows a negative temperature coefficient of electrical resistance, whereas the coefficient of bulk bismuth is positive[3][4]. As the resistance of a very thin film increases gradually for some time after evaporation, the measurement must be made after the resistance has reached a constant value. Thicker films, however, exhibit little or no change in resistance with time. In the present experiments the measurement were carried out after the specimen had been exposed to air for twenty hours or more. During the measurement the electric current through the specimen must be kept as small as possible, otherwise, owing to the rising of temperature

3) M. Czerny, W. Kofink und W. Lippert: Ann. d. Phys. **8** (1950) 65.
4) H. Reimann: Ann. d. Phys. **16** (1955) 52.

caused by the current, the resistance of the bolometer would change considerably.

The thickness d of the bolometer strip was calculated by the following formula

$$d=\frac{1}{4\pi r^2}\frac{M}{\rho}$$

where r is the distance between the collodion membrane and the tungsten coil, M the mass of the substance evaporated and ρ its density. This value means nothing but a rough measure of the thickness of the film.

When the thickness of the evaporated film is less than 1000 A, the variation of electrical resistance with temperature exhibits a fairly large hysteresis and its value is not reproducible. Generally the reistance tends to decrease after repeated measurements. This hysteresis becomes less marked with increase of film thickness, and if the thickness exceeds about 3000 A the hysteresis disappears completely. The numerical value of the temperature coefficient of electrical resistance becomes greater as the film thickness increases. (Fig. 2)

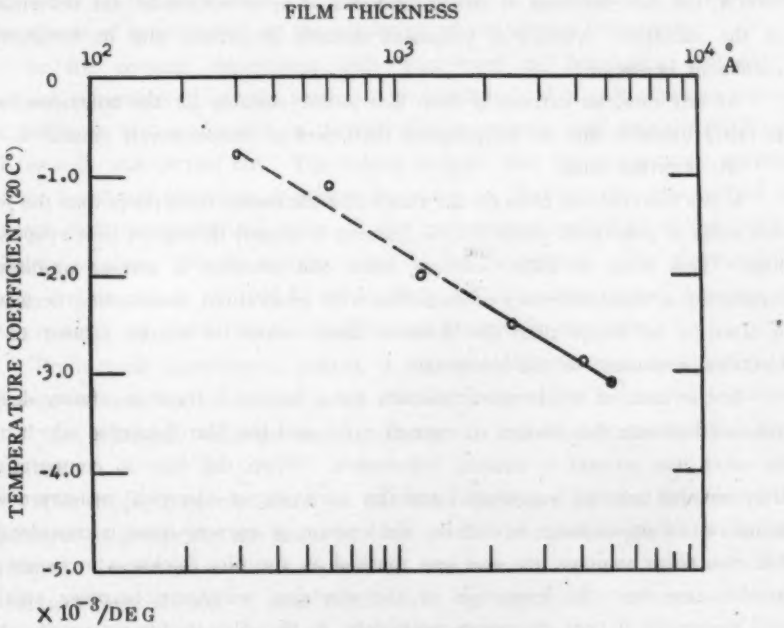

Fig. 2. Temperature Coefficient of Bismuth Film

The broken line in the figure indicates the region in which the variation of

resistance with temperature is not stable. These measurements are in good agreement with those of Reimann, Czerny and others[3][4].

As is well known[5][6], thin evaporated films of most substances are not continuous, but composed of many isolated islands. These islands grow larger as the film thickness increases and come in contact with one another if the thickness becomes several hundred angstroms. Though such films can be regarded as almost continuous, they are still not very strong and are liable to be deformed by the action of external forces. Their structure may be also appreciably different from that of bulk substances, for the structure of evaporated films is often influenced by the nature of substrates.

If the temperature of these films changes, an irreversible change will take place as the result of recrystalization and expansion or contraction of the collodion membrane used as substrate. For these reasons, the electrical resistance and accordingly the temperature coefficient of the evaporated film which is thinner than about 1000 A are not unique, but exhibit different values in each measurement. On the other hand, if the thickness of the film exceeds about 3000 A, the film becomes so strong and stable as to withstand the deformation of the substrate, whence it possesses definite properties and its temperature coefficient is unique.

At any rate, an extremely thin film is not suitable for the bolometer, as it is fairly unstable and its temperature coefficient is comparatively small.

(B) Current noise

It has been noticed from earlier times that the excess noise other than the Johnson noise is generated when electric current is passed through a thin evaporated film. This noise is called current noise and presents a serious problem in measuring a small intensity of radiation with evaporated bolometers, because it is often by far larger than the Johnson noise which is simply related to the electrical resistance of the bolometer.

In the case of evaporated bismuth films, however, there is afairly definite relation between the amount of current noise and the film thickness which must be taken into account in making bolometers. When the film is comparatively thin (several hundred angstroms) and the variation of electrical resistance with temperature shows large hysteresis, the amount of current noise is considerable, but this noise becomes less and less marked as the film thickness increases and at the same time the hysteresis of the electrical resistance becomes smaller, and eventually it does disappear completely if the film thickness exceeds about

5) R. G. Picard and O. S. Duffendack: J. Appl. Phys. **14** (1943) 291.
6) H. Levingstein, J: Appl. Phys. **20** (1949) 306.

3000 A. On the other hand, the evaporated film of bismuth is liable to be crumpled when the collodion membrane used as the substrate is too thin, and as such a film shows also an appreciable current noise, the thickness of the collodion membrane must be greater than about 2000 A.

Thus the evaporated bolometer strip suitable for a delicate measurement of radiation must be considerably thick and strong. It is generally believed that evaporated bolometers have no definite properties and is not suitable for accurate measurement on account of their instability, but this is not the case with the thick bolometer strips stated above if they are carefully constructed.

(C) Effect of sensitization

Experiments have given evidence which indicates that, when the atoms (or molecules) evaporated from an oven in vacuum condense on a surface forming a thin film, the film formation is facilitated if there exist suitable nuclei on that surface. This is because the atoms are immediately trapped by these nuclei and grow into micro-crystals. This phenomenon is generally known as sensitization[7]. As the structure of films and also their electrical properties are markedly influenced by the presence of a sensitizing layer, it is interesting to investigate the effects of sensitization on the properties of evaporated bolometers.

In the present experiment gold was used as sensitizing material in amount equivalent to several tenths of a monolayer. Actually, a proper amount of gold was first evaporated on the collodion membrane, and then the distillation of bismuth was carried out. The results indicate that the temperature variation of the sensitized bolometer is almost the same as that of the unsensitized one except that the numerical value of the temperature coefficient of resistance is slightly smaller. But the current noise is greatly reduced. The sensitized film with the thickness of 1000 A shows little or no current noise, whereas the unsensitized one gives rise to a fairly large amount of the noise.

From these experimental results, it may be concluded that, as a whole, the process of sensitization improves the characteristics of the evaporated bolometer.

(2) Bolometer strip on the membrane of collodion made by the second method.

The temperature coefficient of electrical resistance of the bolometers thus prepared is practically the same as that of the bolometers made by the first method. Its variation with temperature, however, is not reversible even if the thickness exceeds 5000 A, and furthermore an appreciable amount of current noise is still observed with these very thick films.

7) O. S. Heavens: Optical Properties of Thin Solid Films (1955) 38.

This is perhaps because the tension of the collodion membrane is too strong and destroys the evaporated film when it expands or contracts by the change of temperature or humidity. Hence these bolometers are inferior to those made by the first method.

4. Bolometers of Tellurium

Being a semi-conductor, tellurium seems to be very promising for the bolometer because its temperature coefficient of electrical resistance is much higher than that of ordinary metals. The problem is, however, much more complicated than first expected, for the evaporated film of tellurium shows unusual behaviour[3].

(1) Bolometer strip on the membrane of collodion made by the first method.

Without sensitization the evaporated film is quite unstable and does not show any definite property. If the specimen is heated gradually, its electrical resistance increases abruptly at about 30°C, and after this discontinuous change its variation with temperature exhibits some regularity, but is not at all reproducible. Its large hysteresis makes it almost meaningless to calculate the temperature coefficient. Furthermore, the current noise is so considerable that such a film is quite inadequate to the bolometer for the measurement of radiant energy.

But the evaporated film becomes remarkably stable if the same sensitization as in the case of bismuth is carried out, and those sensitized films thicker than a certain value give reproducible variation of resistance with temperature,

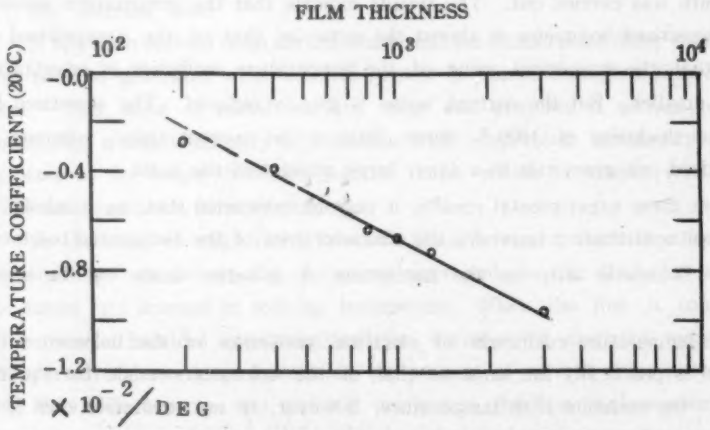

Fig. 3. Temperature Coefficient of Sensitized Tellurium Film

8) K. Yosihara: Memoirs of the Faculty of Engineering, Nagoya University **7** (1955) 81.

showing no trace of hysteresis. This critical thickness seems to depend on the purity of tellurium, and when tellurium from the Merck & Co. is used with the sensitization, it was about 500 A.

It is found that, if the temperature coefficients of resistance of films with various thicknesses are plotted against the thickness, the curve is fairly regular as is shown in Fig. 3, provided these films are produced under the same condition. Such a regularlity cannot be seen for unsensitized tellurium films.

The amount of current noise of the sensitized film is by far less than that of the similar film which is not sensitized, but still, it is more than the Johnson noise. With all the efforts to eliminate this noise, it turned out impossible to obtain any bolometer free from current noise. Thus it was concluded finally that bolometers made of tellurium is in fact inferior to those using bismuth.

(2) Bolometer strip on the collodion film made by the second method.

As the variation of reistance with temperature for the unsensitized film shows some regularity, it is possible to make a rough estimation of the temperature coefficient. The coefficient is plotted against the film thickness in Fig. 4. Here, in contrast to the above-stated case, the numerical value of the tem-

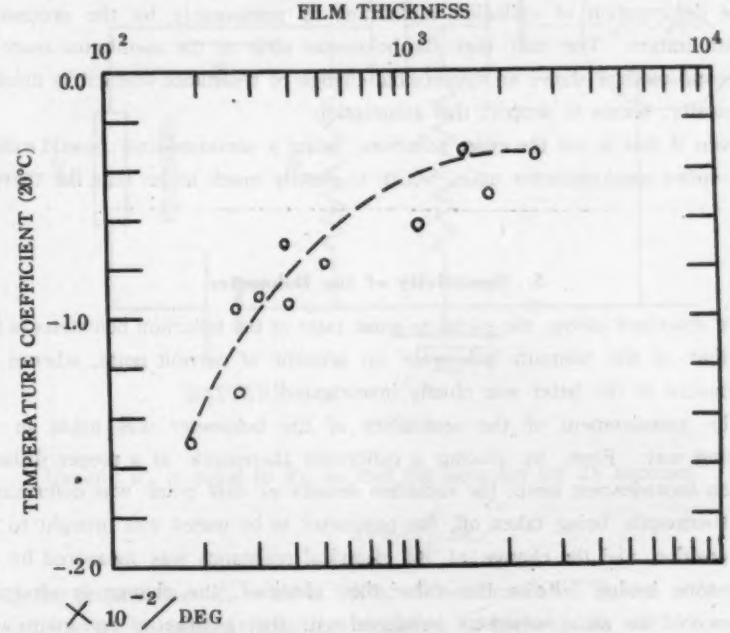

Fig. 4. Temperature Coefficient of Tellurium Film

perature coefficient becomes larger with decrease of the film thickness.

The current noise decreases slightly with increase of the film thickness until the thickness attains to 1500 A. A sudden increase of noise, however, is observed when the thickness exceeds about 1500 A, which makes the film quite useless for the bolometer. At any rate, all these tellurium bolometers, even if the film is thinner than 1500 A, generate more current noise than the best bismuth bolometer.

(3) Origin of current noise in tellurium film.

The reason why the tellurium film shows a large current noise, may be the following.

As tellurium is an exceedingly brittle substance, its evaporated film is neither strong nor stable, and is easily damaged by the action of external forces, for example, by the deformation of collodion membrane. This gives rise to many points of imperfect electrical contact in the film, which makes the origin of current noise when electric current is passed through it. The abrupt change of electrical resistance at about 30°C in the tellurium film described above in the section (1) suggests that the film is broken into small pieces at this temperature by the deformation of collodion membrane or presumably by the process of recrystallization. The fact that the bolometer strip on the membrane made by the second method shows an appreciable change of resistance when it is dried in a dessicator, seems to support this assumption.

Even if this is not the case, tellurium, being a semiconductor, would exhibit the so-called semiconductor noise, which is usually much larger than the thermal noise.

5. Sensitivity of the Bolometer

As described above, the signal-to-noise ratio of the tellurium bolometer is less than that of the bismuth bolometer on account of current noise, whence the performance of the latter was chiefly investigated.

The measurement of the sensitivity of the bolometer was made in the following way. First, by placing a calibrated thermopile at a proper distance from an incandescent lamp, the radiation density at this point was determined. This thermopile being taken off, the bolometer to be tested was brought to the same position, and the change of its electrical resistance was measured by the Wheatstone bridge. From the value thus obtained, the change in electrical resistance of the same bolometer irradiated with the radiation of one micro-watt can be easily calculated. In this measurement, a suitable diaphragm must be

placed directly in front of the bolometer in order to avoid the warming up of the bolometer housing by the radiation. But it is difficult to eliminate zero drift completely, and the results obtained are not very accurate.

In actual measurement of radiation a resistance (or an inductance) is inserted in series to the bolometer, and the variation of voltage across this resistance is amplified with a suitable amplifier. (Fig. 5) This variation of voltage ΔV is given by

$$\Delta V=-I\frac{R_S}{R_B+R_S}\Delta R_B$$

where I is the electric current through the circuit, R_B and R_S are the resistances of the bolometer and the series resistance respectively and ΔR_B is the change of the bolometer resistance caused by radiation.

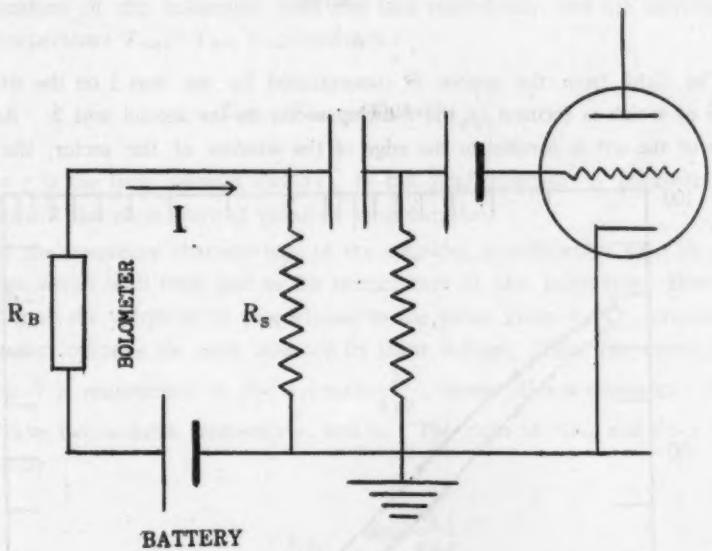

Fig. 5.

Usually R_B is equal to R_S, so that the equation for ΔV becomes

$$\Delta V=-\frac{I}{2}\Delta R_S$$

In the present case R_B is about 1 KΩ. When irradiated by one micro-watt, the value of ΔV calculated from this equation is between 20 and 30 micro-volts, provided the electric current I is 2 milliamperes. On the other hand, as the

bolometer is damaged if the current exceeds 10 milliamperes in the atmosphere of about 15°C, its maximum sensitivity would be much higher.

6. Frequency Characteristics of the Bolometer

The arrangement as shown in Fig. 6 was used to determine the frequency characteristics of the bolometer.

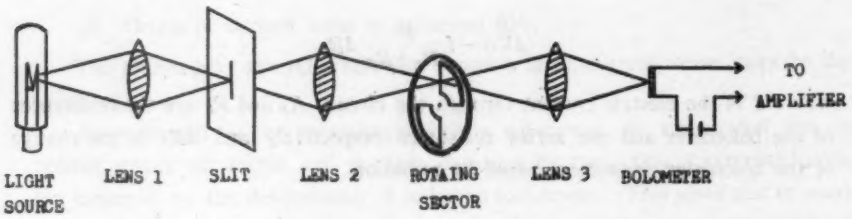

Fig. 6

The light from the source is concentrated by the lens 1 on the slit, the image of which is focused on the rotating sector by the second lens 2. As the image of the slit is parallel to the edge of the window of the sector, the light

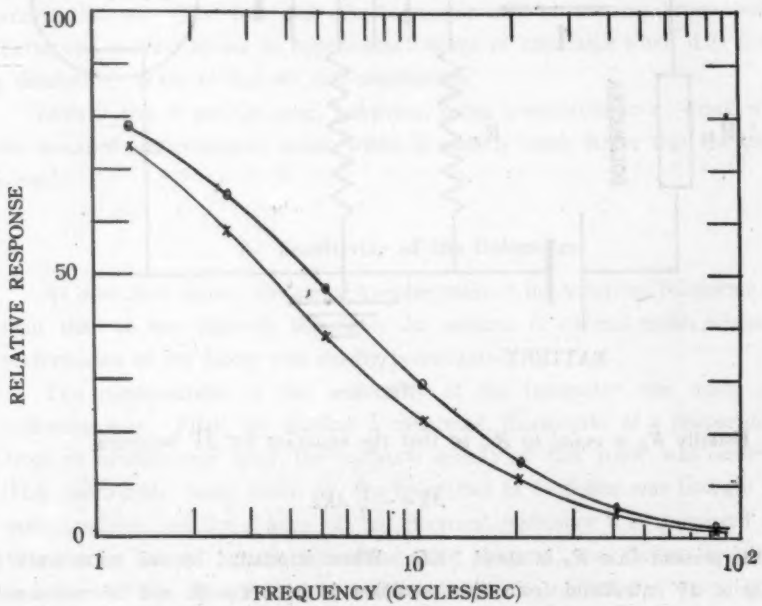

Fig. 7. Frequency Characteristics of the Bolometer

beam appears and is cut off instantaneously, generating rectangularly modulated light pulses. This is necessary to define the wave form of the signal. This light pulse is focused on the bolometer by another lens 3. The output of the bolometer is amplified with a wide range amplifier, rectified and measured with a vacuum tube voltmeter. The characteristics of the amplifier and the voltmeter were previously cheked using a phototube instead of the bolometer. In Fig. 7 the output of the amplifier is plotted against the frequency of modulation for two bolometers in air. Because both the bismuth film and the collodion membrane are made comparatively thick in order to eliminate the current noise and to increase the temperature coefficient of resistance, the frequency characteristics is not so satisfactory as expected.

The time constant of the bolometer was calculated as follows.

If in unit time, ν light pulses impinge on the bolometer successively, the temperature of the bolometer rises and falls periodically, and the amplitude of the temperature $T_{max}-T_{min}$ is given by

$$T_{max}-T_{min}=\Delta T_{\infty}\tanh\frac{1}{4\nu\tau} \qquad (3)$$

where τ is the time constant and ΔT_{∞} is the final increase in bolometer temperature if the pluse were of infinitely long duration.

If the frequency characteristic of the amplifier is sufficiently flat, its output voltage varies with time just as the temperature of the bolometer. Hence, the reading of the voltmeter is proportional to the value given by (3), provided the voltmeter indicates the peak value of its input voltage. Thus the curve shown in Fig. 7 is represented by $f(\nu)=A\tanh\frac{1}{4\nu\tau}$, where A is a constant.

Take two suitable frequency ν_1 and ν_2. The ratio of $f(\nu_2)$ and $f(\nu_1)$ is then given by

$$\frac{f(\nu_2)}{f(\nu_1)}=\frac{\tanh\frac{1}{4\nu_2\tau}}{\tanh\frac{1}{4\nu_1\tau}}$$

which does not contain A, and is a function of τ only. This function can be plotted easily using the tables of hyperbolic functions. (Fig. 8)

In the present case ν_1 and ν_2 are 1.5 and 5 cycles/sec. respectively. The ratio $f(\nu_2)/f(\nu_1)$ of the acutual bolometer can be obtained from the curve in Fig. 7. From this value, the time constant of the bolometer is determined

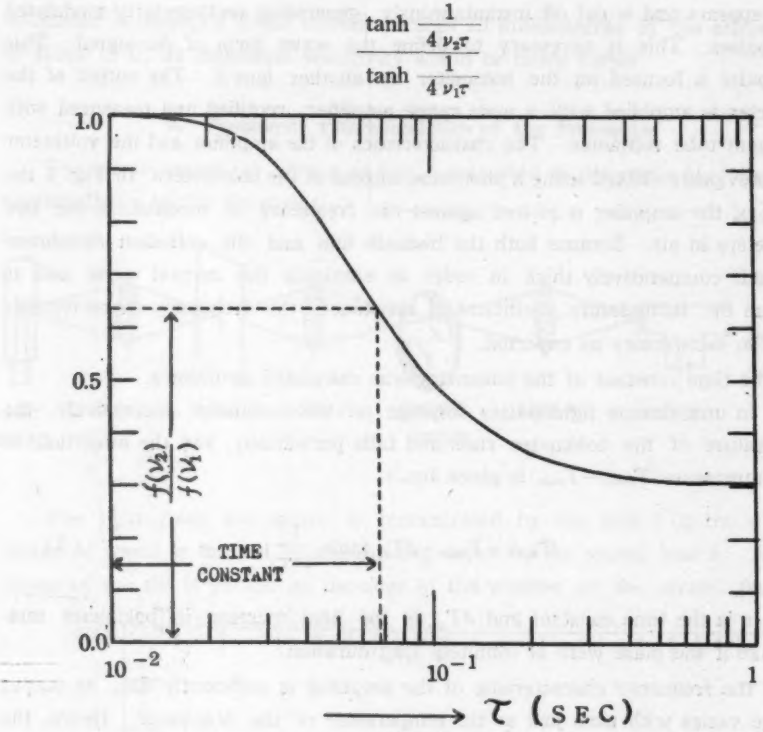

Fig. 8

graphically as shown in Fig. 8. The bolometers, the characteristics of which are plotted in Fig. 7, have the time constants of 68 and 85 milliseconds respectively.

7. Performance of the Bolometer

The bismuth bolometer stated above was used as the detector of an infra-red spectrometer, and recordings of typical infra-red spectra were made to test its actual performance.

The current through the bolometer was 2 milliamperes supplied by a 4 volts storage battery. The radiation from the source was chopped by a rotating sector and signals of 10 cycles per sec. were generated. The output of the bolometer was first amplified with an input transformer and then with a conventional tuned voltage amplifier which was carefully constructed to eliminate undesirable noise. The output of the amplifier was rectified synchronously with a mechanical rectifier and then supplied to a galvanometer. The deflection of the galvanometer

was recorded on a photographic paper with a simple self-recording device.

The spectrometer was one of Litrow type equipped with a LiF prism of the surface $6 \times 4.5\,cm^2$. The focal length of its collimator mirror was 52.5 cm. As the entrance slit was linear, its height was reduced within 10 mm to avoid the lowering of resolving power owing to the curvature of its image on the exit slit. This situation, with the relatively small size of the prism employed, made the available radiation energy considerably limited, whence the recording time had to be lengthened in order to secure good resolution of the spectrum.

Fig. 9 shows the absorption spectrum of HCl in the region of 3.5 μ. The fine structure due to rotation is clearly observed.

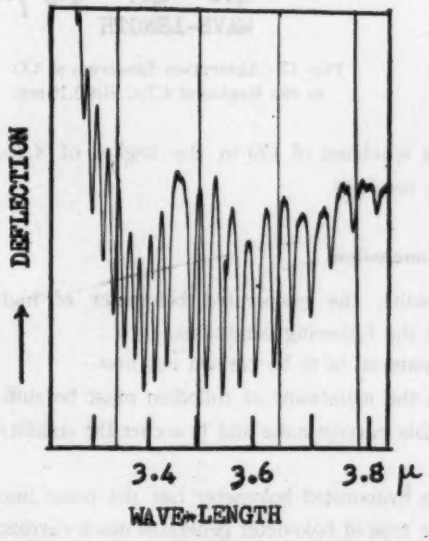

Fig. 9 Absorption Spectrum of HCl in the Region of 3.5 μ, Slit 0.16 mm

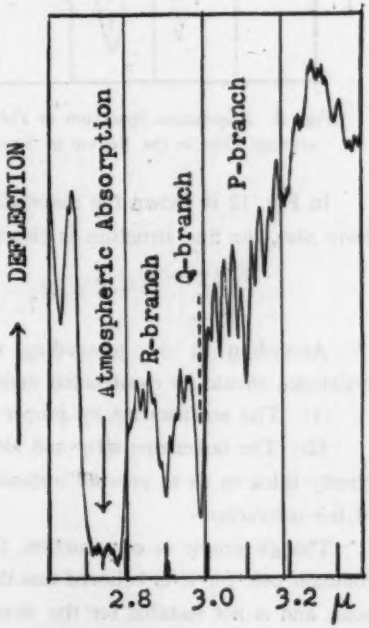

Fig. 10 Absorption Spectrum of NH_3 in the Region of 3.0 μ, Slit 0.15 mm

Fig. 10 is the absorption band of NH_3 at 3μ. The fine structure is fairly well resolved though it is not so distinct as in the case of HCl. The R-branch is somewhat obscured on account of the overlapping of the interference fringe by the mica window of the bolometer housing.

Fig. 11 is the absorption spectrum of polystyrene film with the thickness of of about 30μ, which is often used for the calibration of wavelength.

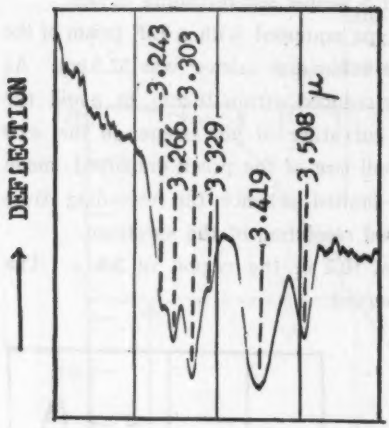

Fig. 11 Absorption Spectrum of Polystyrene Film in the Region of 3.4μ

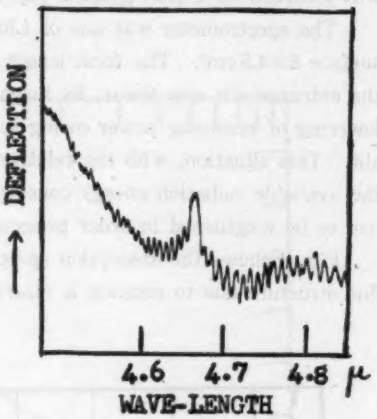

Fig. 12 Absorption Spectrum of CO in the Region of 4.7μ, Slit 0.15 mm

In Fig. 12 is shown the absorption spectrum of CO in the region of 4.7μ. Here also, the fine structure is clearly resolved.

7. Conclusion

According to the preceeding results, the evaporated bolometer of high resistance should be constructed under the following conditions.

(1) The sensitization by proper material is to be carried out first.

(2) The bolometer strip and also the membrane of collodion must be sufficiently thick so as to prevent undesirable current noise and to secure the stability of the bolometer.

Though simple in construction, the evaporated bolometer has not come into common use, for it is believed that this type of bolometer generates much current noise and is not suitable for the detector of a spectrometer. This is because the origin of the current noise was not well understood and accordingly the method of construction was inadequate. The recordings of infra-red spectra in the preceding section show clearly that the evaporated bolometer works as successfully as any other infra-red detector. Furthermore, the high sensitivity as well as the high resistance of this bolometer makes it possible to reduce the turn-ratio of the input transformer, and in fact, even the ordinary input transformer not specially constructed for the infra-red work is often sufficient for the usual measurement of infra-red spectra, if only precautions are taken to

shield it from stray magnetic fluxes. This is a very favourable condition, leading to the simplification of the amplifying system which is usually fairly delicate.

From these considerations the evaporated bolometer with high resistance may be recommended in many fields of infra-red work.

8. Acknowledgement

The author wishes to express his appreciation to Prof. T. Suga for his kind guidance and encouragement thoroughout this work.

Production of Replica Gratings I

Masao SEYA and Katsuya GOTO

Institute for Optical Research, Tokyo University of Education

(Received June 23, 1956)

Abstract

Several methods for the production of replica gratings have been reported, but no papers have been written about the detail of stripping method of Aluminium film deposited by evaporation on the grating surface. The technique of the production and the quality of replica gratings by this method are studied.

1. Introduction

Fifty years have gone by since the replica grating was first made. During these years, several methods have been applied for the production which are classified as

1) Collodion method[1)2)],
2) Stripping of vacuum evaporated aluminium film[3)4)],
3) Artificial resin casting[5)].

The first method, which is most commonly used and has been studied by many workers, seems to involve some difficulty in producing good replicas. The third method is suitable for transmission replicas but not for reflection replicas. As for the second method, R. W. Wood[3)] and R. A. Sawyer[4)] wrote only a few lines in their papers and no papers seem to have ever been written about the detail of the method. The authors undertook the study of the second method to learn its technique and to test the replicas thereby produced.

2. Method of Production

As the mother grating, the following three were used:

1) A grating ruled on speculum metal (ruled by Dr. Y. Sakayanagi),

1) T. Takamine and H. Ono: J. Appl. Phys. Japan **14** (1945) 12.
2) G. D. Dew and L. A. Sayce: Proc. Roy. Soc. London **207** (1951) 278.
3) R. W. Wood: J. Opt. Soc. Amer. **36** (1946) 715.
4) R. A. Sawyer: Experimental Spectroscopy 1951 p. 150.
5) H. Kubota and Y. Yatabe: J. Appl. Phys. Japan **16** (1947) 123.

2) A grating ruled on aluminium surface deposited by evaporation on a glass plate (ruled by Dr. Y. Sakayanagi),

3) A replica grating produced by the authors' method.

The speculum grating is most suitable as the mother grating. In the case of the aluminium grating, there is more or less a risk of its surface being peeled off during the process of replica making, and with the replica grating, its grooves are liable to be deformed by the radiant heat of the evaporation.

Prior to the evaporation process, it is desirable to clean the surface of the mother grating which is however not always necessary, for the process of production itself makes it remain clean, ready for the next replica.

The coating process needs some care. To minimize the effect of radiant heat, a shutter was provided which was opened when the evaporation started and closed when the film thickness became sufficient. There is no strict limitation in the thickness of the film. Aluminium was used as the coating material because of its low boiling point and good reflecting power. At first, it was feared that depositing aluminium over aluminium might result in damaging the original by being peeled off from the glass plate. But all went well even with a very clean state of the surface.

After the deposition, a glass plate was laid on the coated grating with Epikote resin 828 (promoter: diethylene triamine) as adhesive and kept pressed down by a weight. Epikote resin has a better adhesive power than acryl resin that was tried first. The polymerization was carried out in a thermostat. Epikote resin is transparent, but when mixed with the promoter, it turned milky by the occlusion of small air bubbles which were removed by warming the mixture to 40–50°C under a reduced pressure. Before pouring the resin on to the coating, the latter and the glass plate were warmed up to the temperature of polymerization. The resin should be used as little as possible to form a thin film. After the completion of the polymerization, which was checked separately by a test tube trial using the same resin, the replica was detached from the mother grating, the process of which would require some effort if the grating area is large. In the present case, the ruled area was 35 mm × 50 mm and a simple tool was all that was used for detaching. The detaching should be performed before the temperature drops below that of the polymerization, especially when a speculum grating is used, for the difference in thermal expansion between the speculum and the glass plate may cause the latter to crack when cooled as frequently experienced by the authors. As for the glass plate, a piece of thick commercial plate glass was good enough for the present purpose.

By using a speculum concave grating and preparing a set of convex and

concave glass surfaces of the same radius of curvature as that of the grating, a concave replica was made by the same technique first by making a convex replica then a concave one from it.

3. Result

Using the first replica as the mother for the second and so on, a fifth replica was made. The accompanying figure shows the comparison of arc spectra obtained by the original grating and the fifth replica. The resolving power of the fifth does not seem to be inferior to that of the original.

Thus, with this method, every replica can be used as the mother for the next which is of great advantage over the collodion method.

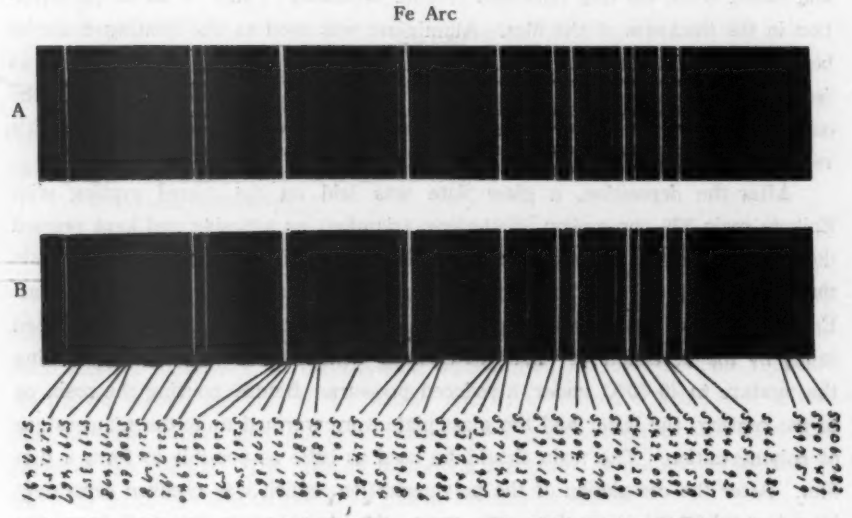

Fig. 1. A; Original Grating B; The Fifth Replica Grating

4. Acknowledgement

The authors wish to express their thanks to Dr. Sakayanagi who lent them his gratings for the experiment and to the Institute for Applied Optics for financial support.

Ultraviolet and Infrared Spectra of Phenol-Aromatic Solutions

Yoshiki SATO

Institute for Optical Research, Tokyo University of Education

(Received June 24, 1956)

Abstract

The ultraviolet spectra not found in either of the partners alone are observed for solutions of phenol diluted with benzen, toluene, *o*- and *p*-xylene, from which the extinction coefficients and equilibrium constants of the complexes are estimated. In addition, the first overtone bands of the phenol hydroxyl stretching frequency in the aromatic solutions are obtained, the wave numbers of which are excellently correlated with the ionization potentials of the aromatic molecules. In conformity with these experimental results, geometrical arrangement between phenol and the aromatic molecules are expected to correspond to an "oblique" model O suggested by Mulliken.

1. Introduction

Mecke[1] stated that when benzene and toluene are used as solvent the second overtone band of phenol hydroxyl stretching vibration in dilute solution splits into two components, the frequency of one of which is greatly changed to smaller value than that of the corresponding band in carbon tetrachloride, and suggested that the reason for this would be attributable to strong interaction with π-electrones of double bonds of the solvent. In hydrogen bonding, the importance of delocalization energy of non-bonding electrons, which belong to a proton acceptor atom taking part directly in the hydrogen bonding, has been stressed by several workers[2][3][4], and a few infrared absorption studies which may be considered to support their theories have been made[5][6].

On the other hand, since Benesi and Hildebrand[7], using ultraviolet absorption

1) R. Mecke: Disc. Farady Soc. No. **9** (1950) 161.
2) K. Nukasawa, J. Tanaka and S. Nakakura: J. Phys. Soc. Japan **8** (1953) 792.
3) H. Tsubomura: Bull. Chem. Soc. Japan **27** (1954) 445.
4) C. A. Coulson and U. Danielson: Ark. Fys. **8** (1954) 239, 245.
5) Y. Sato and S. Nagakura: Science of Light [Tokyo] **4** (1955) 120.
6) H. Tsubomura: J. Chem. Phys. **23** (1955) 2130: 24 (1956) 927.
7) H. A. Benesi and J. H. Hildebrand: J. Am. Chem. Soc. **70** (1948) 2703.

methods, showed definitely that benzene forms 1:1 complex of considerable stability with iodine, a great number of molecular complexes have been investigated by this spectroscopic method. In order to explain the mechanism of the appearance of ultraviolet spectra characteristic of the molecular complexes, Mulliken[8], in 1951, introduced his famous intermolecular charge-transfer theory.

The author in his ultraviolet absorption study of diluted phenol-aromatic mixtures observed particular bands not found in either of the partners alone, from which molar extinction coefficients and equilibrium constants of the complexes were estimated. In addition, the first overtone bands of the phenol hydroxyl stretching vibration in the aromatic solvents, using a near infrared grating spectrometer, were also measured in detail. As a result, it was found that there is an excellent correlation between the wave numbers of the hydroxyl stretching absorption bands and the ionization potentials of the aromatic molecules.

In this paper, interaction between phenol and the aromatic molecules is discussed in conformity with these experimental results.

2. Experimental and Results

Phenol was used as electron acceptor (according to Mulliken's theory), and several aromatic molecules, i.e., benzene, toluene, *o*-, and *p*-xylene as electron donor. Carbon tetrachloride, in measurements of ultraviolet spectra, was mainly used as solvent, but specific influences of solvent upon the ultraviolet spectra were checked by using n-heptane solution instead of carbon tetrachloride solution. These substances are all of special grade and were found to contain less impurities than could be detected spectroscopically. These were not further purified. The extinction coefficients of the ultraviolet spectra were measured with a Hitachi model EPU-2 spectrophotometer, using quartz cells of 10 mm thickness for all the measurements. The infrared spectra were obtained with the instruments previously described in earlier papers[9].

Since the extinction coefficients of the ultraviolet spectra in question are very small as shown below and also the transparency of phenol is considerably small in this wavelength range, the author, then, determined optical densities of the ultraviolet spectra characteristic of the phenol-aromatic complexes by the following way: the optical densities of the aromatic molecules in dilute solutions were subtracted from those of the phenol and aromatic molecules in dilute solutions, the latter

8) R. S. Mulliken: J. Am. Chem. Soc. **74** (1952) 811.
9) See, for example, reference (5).

of which were measured by using diluted phenol solution as a reference. Recording the optical densities thus obtained against the wavelength in mμ for all the phenol-aromatic complexes, we have Fig. 1, in which an arbitrary scale is employed for each curve. In Table 1, the second column represents the wavelength λ_{max} of the peak of each curve indicated in Fig. 1.

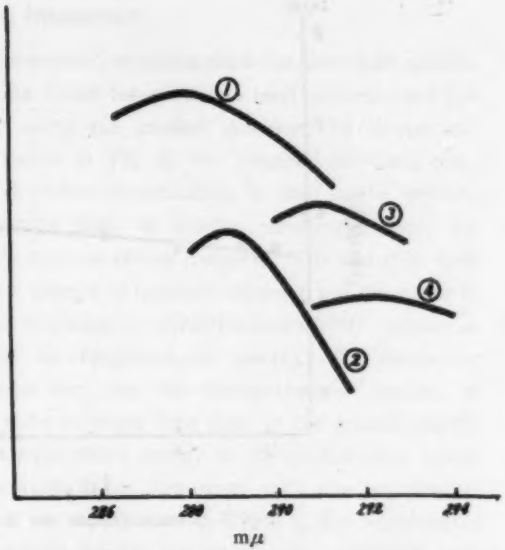

Fig. 1. Schematic diagram of ultraviolet spectra of the various complexes: (1) benzene-phenol, (2) toluene-phenol, (3) *o*-xylene-phenol, (4) *p*-xylene-phenol.

As shown by Benesi and Hildebrand[7], plotting $[A]l/d$ against $1/[B]$, where $[B]$ and $[A]$ are respectively the molar concentration of the aromatic molecules and that of phenol, and l and d respectivelys are the cell length and the optical density determined as above, straight lines, as, for example, illustrated in Fig. 2 for the phenol-benzene complex, are also obtained for all the other complexes. When *o*- and *p*-xylene are used as the electron donor, it is difficult to obtain accurate straight lines, since in these cases $[B]$ cannot be taken to satisfy the condition $[A \cdot B] \ll [B]$, in which $[A \cdot B]$ is the molar concentration of the complex, because of the smallness of their own transpararency. From the above-described results, it is concluded that there is a 1:1 complex formation between phenol and all the aromatic molecules used.

Table 1. Ultraviolet and infrared spectral data of the phenol-aromatic complexes, and ionization potentials of the aromatic molecules.

Donor	λ_{max} (mμ)	ν_{max} (cm^{-1})	$\nu_{cl_4} - \nu_{max}$ (cm^{-1})	I_p (eV)
Benzene	288	6925	115	9.24
Toluene	289	6915	125	8.82
o-Xylene	291	6904	136	8.58
p-Xylene	292	6899	141	8.48

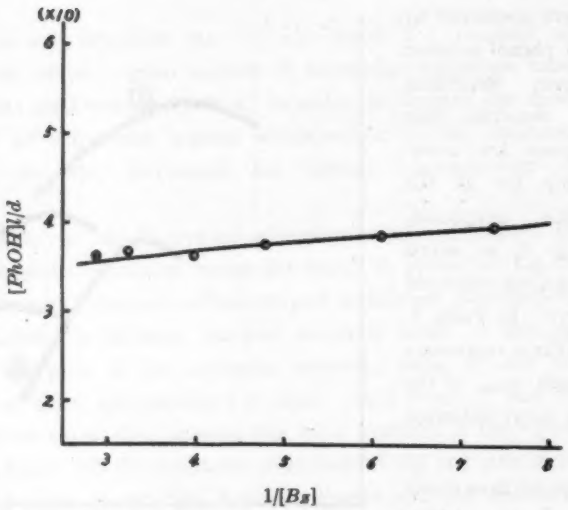

Fig. 2. Concentrations are in moles/liter.

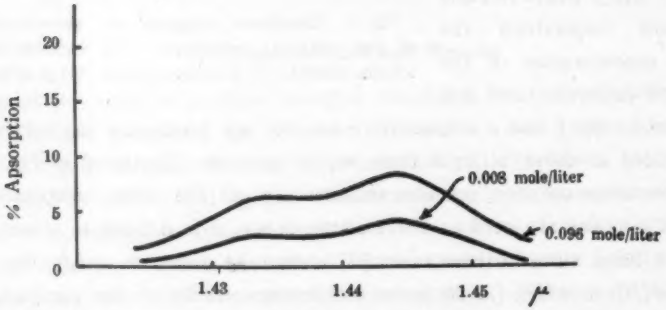

Fig. 3. The first overtone band of phenol stretching vibration in benzene solution.

In addition, using a near infrared grating spectrometer, the first overtone bands of the hydroxyl stretching vibration, the second overtone bands of which in benzene and toluene solutions were observed previously by Luttke and Mecke[1], were investigated by the use of all the aromatic molecules listed in the first column of Table 1 as solvents. As an illustration, Fig. 3 shows the hydroxyl absorption band of phenol in benzene solution. In Table 1, the third column gives the wave numbers, ν_{max}, of the absorption peak of the lower frequency components, the fourth column the wave number differences between ν_{max} and the corresponding ones in carbon tetrachloride solution, and the fifth column the ionization potentials of the aromatic molecules.

3. Discussions

As seen in Fig. 1, all the phenol-aromatic complexes show the ultraviolet spectra characteristic of them, which are not found for phenol in inert solvents, nor for the aromatic molecules. Moreover, using the method described by Benesi and Hildebrand, the straight lines, as shown in Fig. 2, are obtained for these complexes. When n-heptane, instead of carbon tetrachloride, is used as the solvent, the afore-mentioned ultraviolet spectra shift to shorter wavelength side, for example, appearing at 284 mμ for the benzene-phenol complex. The fact that such slight solvent shift of the ultraviolet spectra in question occurs when the medium is altered, being almost certainly due to change in refractive index[10)11)12)], allows us to consider that these spectra may be charge-transfer spectra. The reason for this is explained by the well-known fact that the charge-transfer spectra, in which the polarity of the excited state is larger than that of the ground state[8)], shift in consequence of the larger stabilization energy of the excited state, which is due to the polarization of the solvent, when compared with the stabilization energy of the ground state. Also, as clearly seen in Table 1, the wavelengths of the absorption peak of the ultraviolet spectra are excellently correlated with species of the donor molecules, that is, λ_{max} becomes larger as one proceeds from benzene through toluene and *o*-xylene to *p*-xylene, in other words, with decreasing ionization potentials of the aromatic molecules. Such behaviour has been pointed out previously by several workers[13)14)] for molecular complexes, and interpreted on the basis of Mulliken's charge-transfer theory. Recently, similar regularity has also been recognized by Kuboyama and Nagakura[15)] in their study of *p*-benzoquinone-aromatic complexes, and was clearly understood from the viewpoint of the "molecular energy-level diagram" introduced by Nagakura and Tanaka[16)].

In view of the foregoing facts it seems necessary to consider the mechanism of the appearance of the charge-transfer spectra in question. For example, in the p-benzoquinone-aromatic complexes previously described, the charge-transfer spectra characteristic of these complexes should be interpreted as due to the transfer of an electron from the highest occupied orbital of the aromatic molecules to the lowest vacant orbital of *p*-benzoquinone. As clearly shown in Table

10) N. S. Bayliss: J. Chem. Phys. **18** (1950) 292.
11) N. S. Bayliss and E. G. McRac: Phys Chem. **58** (1954) 1002.
12) J. S. Ham: J. Am. Chem. Soc. **76** (1954) 3881.
13) H. McConnell, J. S. Ham, and J. R. Platt: J. Chem. Phys. **21** (1953).
14) S. H. Hastings, J. L. Franklin, J. C. Schiller and F. A. Matsen: J. Am. Chem. Soc. **75** (1953) 2900.
15) A. Kuboyama and S. Nagakura: J. Chem. Soc. Japan **75** (1955) 1082, J. Am. Chem. Soc. **77** (1955) 2644.
16) S. Nagakura and J. Tanaka: J. Chem. Phys. **22** (1954) 236.

1, there is, as is the case of the ultraviolet spectra, an excellent relationship between the wave numbers of the absorption peak of the phenol hydroxyl stretching bands and the ionization potentials of the aromatic molecules, that is, the former decreases as the latter decreases. This remarkable behaviour may be interpreted by assuming that an electron migrates, in the formation of the complex or hydrogen bonding, from the highest occupied orbital of the aromatic molecule to the antibonding orbital of the OH radical of phenol. The fact that no ultraviolet spectra corresponding to those in phenol-benzene solution appear in anisole-benzene solution, may support the above descriptions. At this stage, it seems reasonable to assume that the relative configuration between the OH radical of phenol and the aromatic molecules corresponds to an "oblique" model O suggested by Mulliken. In complex, we must take into account such non-reasonance interaction as electrostatic and dipole-induced dipole interactions as well as the reasonance interaction as above. As to the polarity of the CH link, Coulson[17] concluded it theoretically to be $C^+—H^-$. On the other hand, Thompson et al.[18][19] gave the reverse polarity, which agrees with the generally accepted view, through infrared intensity measurements of bending vibrations of substituted benzenes. According to the latter's conclusion, as polarities of benzene rings of the phenol and aromatic molecules are both negative, the electrostatic repulsive force acts between both benzene rings, while the electrostatic attractive force acts between the OH radical of phenol and the benzene ring of the aromatic molecules. Furthermore, dipole moment of phenol can be regarded to localize to σ link of the OH radical. It seems then likely that the dipole-induced dipole interaction mainly acts between the OH radical and the aromatic molecules. From these considerations, the above-mentioned geometrical configuration between phenol and the aromatic molecules may likely be understood. Also, as can easily be shown, the OH radical cannot attach parallel to the planes of the aromatic molecules. In practice, no OH stretching bands of the aromatic molecules are entirely influenced by the existence of phenol.

Lastly, on the basis of the above-described geometrical arrangement, the intensities of the charge-transfer spectra obtained are to be discussed. According to Mulliken's charge-transfer theory[8], the wave function of the ground state of any molecular complex $A \cdot B$ is given by

$$\psi_N = a\phi_0 + b\psi_1 + \cdots\cdots , \qquad (1)$$

17) C. A. Coulson, Trans. Faraday Soc. **38** (1942) 433.
18) R. P. Bell, H. W. Thompson and E. E. Vago: Proc. Roy. Soc. 192 (1948) 498.
19) A. R. H. Cole and H. W. Thompson: Trans. Farady Soc. **46** (1950) 103.

where ψ_0 represents a "no-bond" wave function $\psi(A\cdot B)$, ψ_1 a "dative" wave function $\psi(A^-\!-\!B^+)$. The higher terms in Eq. (1) represent, for example, the wave function of the state in which an electron migrates from the highest occupied orbital of the aromatic molecule to the lowest vacant orbital of phenol, but it is plausible that usually the first dative term may be predominant. Neglecting the overlapping between the two components, the following approximate relation for the coefficients in Eq. (1) is given by

$$\rho \equiv b/a = -H_{01}/(W_1 - W_0) . \qquad (2)$$

The excited state wave function ψ_E corresponding to Eq. (1) is necessarily expressed by

$$\psi_E = a^*\psi_1 - b^*\psi_0 + \cdots\cdots \qquad (3)$$

with $a^* \approx a$ and $b^* \approx b$. Using Eqs. (1) and (3), the quantum mechanical transition moment μ_{EN} corresponding to the charge-transfer spectra is evaluated as follows:

$$\mu_{EN} \approx a^* b e (r_B - r_A) . \qquad (4)$$

r_B and r_A represent the average positions of the electrons in A and B orbitals respectively from any convenient origin, and e the electronic charge. Frequently, experimental data are expressed in terms of the so-called oscillator strength, which, in our case, can be calculated by the following equation

$$f_{EN} = (8\pi^2 \nu mc/3he^2)\mu_{EN}^2 \approx (4.704 \times 10^{-7})\nu\mu_{EN}^2 , \qquad (5)$$

in which ν, in cm^{-1}, is roughly the wave number at the absorption peak. Furthermore, it is also given by the well-known formula[20]

$$f_{EN} = 4.32 \times 10^{-9} \int \varepsilon d\nu \approx (4.32 \times 10^{-9})\, \varepsilon_{max}\, \Delta\nu \qquad (6)$$

where $\Delta\nu$ is the half-breadth of absorption band. Combining Eqs. (4) and (6) with (5), we have the following expression for ε_{max}.

$$\varepsilon_{max} \approx (1.09.10^2)\, \nu/\Delta\nu \cdot a^{*2} b^2 e^2 (r_B - r_A)^2 . \qquad (7)$$

To estimate K and ε_{max} the equilibrium constant and extinction coefficient of the complex respectively, we extend such a straight line as, for example, shown in Fig. 2 to the vertical axis. The intercept on the $[A]\,l/d$ axis is $1/\varepsilon_{max}$, from which K can be computed. ε_{max} and K for benzene-phenol complex are estimated as 3 and 1.5 respectively, and for the other complexes almost similar values to these have also been found. For the *o*- and *p*-xylene-phenole complexes, they

20) R. S. Mulliken: J. Chem. Phys. **7** (1939) 14.

were estimated less accurate through the reason previously described. At any rate, these extinction coefficients are unusually small compared with those of molecular complexes investigated by other workers, for example, $\varepsilon_{max} \approx 9090$ for benzene-chlorine complex[21]. As the extinction coefficient of the charge-transfer spectra is predicted from Eq. (7), the reason for such anomalous differences should be looked for mainly in H_{01} and $r_B - r_A$, remembering that electron affinities of OH radical and chlorine molecule are 50 kcal/mole and 36 kcal/mole[22] respectively and the half-breadths of the absorption bands may be regarded nearly equal in these cases. Recently, Collin and D'Or[23] observed the infrared band corresponding to the fundamental vibration of chlorine molecule in benzene solution. In view of this new evidence, Mulliken[24] stated that the relative configuration between chlorine molecule and benzene seems likely to correspond to an "oblique" model O, or perhaps an unsymmetrical R model, in which the contribution of the more highly excited dative structures as well as the lowest energy dative term are expected. Contrary to Mulliken's viewpoint, Murakami[25] stated that "there is a possibility that chlorine molecule, in a mixture containing no more than the two components, may be contacting with several benzene molecules, and, from the statistical point of view, even when two Cl atoms in chlorine molecule are interacting with one benzene equivalently, they may be interacting with other benzene non-equivalently". If we assume, as the relative orientation between chlorine molecule and benzene, a symmetrical or at least an unsymmetrical R model, the overlapping between chlorine molecule and benzene seems likely much greater than that between phenol and benzene. In addition, hydrogen atom has several characteristics[2], that is, spherical symmetry of ls orbital, non-existence of any electron pair which would repel π-electrons of the aromatic molecules and smallness in the electronegativity scale of the orbital, hence it would be considered that the OH radical of phenol can approach considerably near to the aromatic molecules, in other words, $r_B - r_A$ in Eq. (4) becomes smaller than that in benzene-chlorine complex. From these considerations, the anomaly in the extinction coefficients may be roughly understood.

The solvent effects upon the dipole moment have been disussed by several investigators[26][27]. The beautiful work by Nagakura and Baba shows that the

21) L. J. Andrews and R. M. Keefer: J. Am. Chem. Soc. Soc. **73** (1951) 462.
22) H. O. Pritchard: Chem. Rev. (1953) 529.
23) J. Collin and L. D'Or: J. Chem. Phys. **23** (1955) 397.
24) R. S. Mulliken: J. Chem. Phys. **23** (1955) 397.
25) H. Murakami: J. Chem. Phys. **23** (1957).
26) K. Higashi: Sci. Pap. Inst. Phys. Chem. Res. [Tokyo] **13** (1934) 1167.
27) S. Nagakura and H. Baba: J. Chem. Soc. Japan **72** (1951) 6.

effect of solvent upon the dipole moment of phenol are mainly attributable to the electron-migration effect of lone-pair electrons, which belong to oxygen atom, towards benzene ring. The degree of the electron-migration which rises from the complex formation is small because of the small overlapping between phenol and benzene. It is then naturally expected a small increament of the dipole moment. By comparing the dipole moments of phenol in various solvents measured by them with one another, the above-mentioned facts would be cleared up.

Another interpretation for the cause of the appearance of the ultraviolet spectra observed in the present experiment, may be to attribute them to forbidden transitions of phenol or the aromatic molecules intensified by strong interaction between the two components. Further experiments are in progress.

Acknowledgement

The authors wishes to express his sincere thanks to Professors Y. Fujioka and H. Ootsuka for their deep interest and to Dr. S. Nagakura, University of Tokyo, for his guidance, encouragement and valuable suggestions offered in the present work.

Basis for Selecting Line-Pairs in Quantitative Spectrochemical Analysis (III) Classification of Some Spectral Lines

Hiroshi IIJIMA

(Technical Research Laboratory, Nippon Steel Tube Co., Ltd.)

(Received June 27, 1956)

Abstract

As an important condition in selecting line-pairs in quantitative spectrochemical analysis, it is made clear that they should be homologous composed at least of ionic line-ionic line or neutral line-neutral line. The spectral line Fe 2689.21A, which is used as an internal standard to the spectral line CrII 2677.16A, has been classified as a neutral line. But this line is not simply neutral, it is a blend of FeI line that is neutral and FeII line that is ionic. FeI 2689.21A line is to be classified as $a^5F_4 - v^5D_5^o$, and it is considered reasonable to classify the line FeII 2689.21A as $b^3P_{3/2} - y^4D_{3/2}^o$, and the homologous feature of the line-pair CrII 2677.16A/ Fe 2689.21A is only apparent in Feussner spark excitation.

I. Introduction

The line-pairs that are used in quantitative spectrochemical analysis are supposed to be homologous, in other words, the difference in excitation potentials (E.P.) between the analysis line and the internal standard line is to be small. However, in quantitative analysis of steel, following exceptional line-pairs have often been used:

(1) SiI 2881.58A / FeII 2880.76A.

(2) CrII 2677.16A / FeI 2689.21A.

In the author's first report[1] it was made clear that the line-pair (1) is unstable and unsuitable for the analysis of Si, whereas the line-pair (2) is stable with reproducible intensity ratio and fit for the analysis of Cr, which makes one wonder whether a line-pair, even if it is of ionic-neutral, can serve the purpose equally good. On this point, the investigation was carried out and found that the line Fe 2689.21A is not a neutral line as given in M.I.T. wavelength tables[2] but, in fact, a blend of FeI and FeII lines, the latter, the ionic line, being

1) H. Iijima: J. Spectro. Soc. Jap., Vol. 4, No. 1 (1956), 7.

2) G. R. Harrison: M.I.T. Wavelength Tables (1939).

predominant in Feussner spark excitation. It was then ascertained that the homologue of every line-pair is after all imperative for the analysis.

II. Experimental

2.1 *Influence of excitation method*

Experiments have shown that the ratio of the intensity of ionic line to the intensity of neutral line is always larger than that in d.c. arc excitation. This leads to the presumption that the line Fe 2689.21A is a blend of FeI and FeII lines.

2.2 *Intensity distribution of spectral lines*

In Feussner spark excitation, the intensity distribution of spectral lines along their paths between electrodes depends on the excitation potential. In Fig. 1,

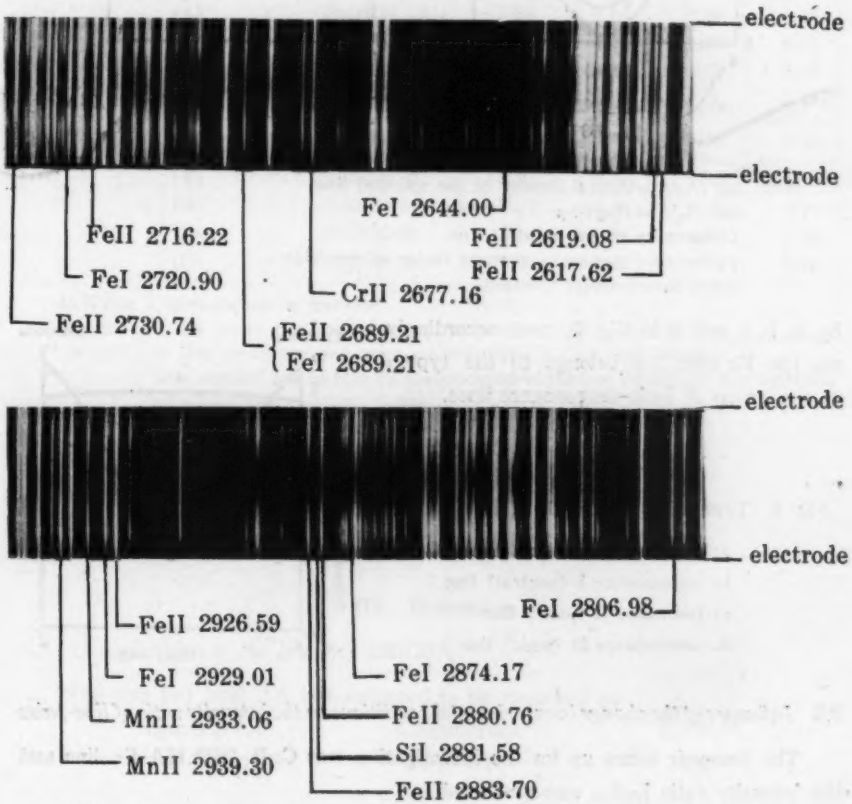

Fig. 1. Qualitative observation on the intensity distributions of various kinds of spectral lines.

iron spectrum is given as an example showing various types of the distribution. For some spectral lines, the distribution was traced with the result shown in Figs. 2(a) and 2(b). There are four types of distribution as indicated

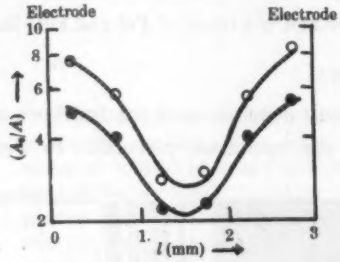

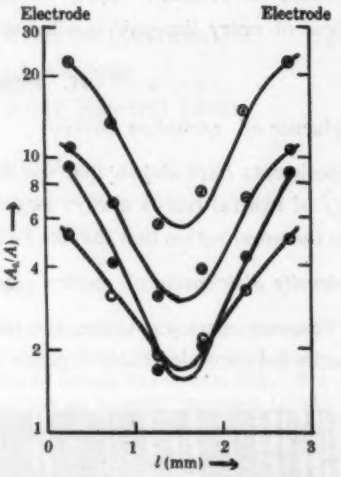

(a) ○ FeII 2926.59A ● Mn 2939.30A (b) ⊙ FeII 2730.74A ⊕ CrII 2677.16A ● FeII 2619.08A ⊙ Fe 2689.21A

Fig. 2. Intensity-distributions of some spectral lines

Note: log (A_0/A)=Optical density of the spectral line
log $(A_0/A)=\gamma \log I+\beta$
I=Intensity of the spectral line
γ=So-called gamma, a contrast factor of emulsion
β=an experimental constant

by a, b, c and d in Fig. 3, and accordingly, the line Fe 2689.21A belongs to the type d of the group of ionic-unresonance lines.

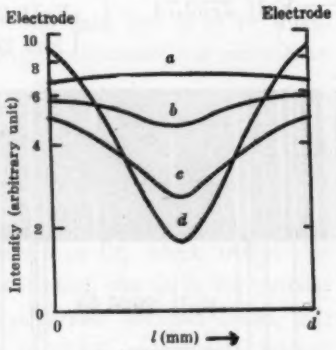

Fig. 3. Types of various kinds of spectral lines.

a: resonance I (neutral) line
b: unresonance I (neutral) line
c: resonance II (ionic) line
d: unresonance II (ionic) line

2.3 *Influence of the change in experimental conditions on the intensity ratio of line-pairs*

The line-pair taken up for the investigation was Cr II 2677.16A-Fe line and the intensity ratio I_{Cr}/I_{Fe} was measured.

In general, changes in electrode gap distance, inductance etc. cause a change

in the intensity ratio in Feussner spark excitation. The extent of the change in the ratio depends on the physical nature of the line-pair and, in the case of I_{Cr}/I_{Fe}, the change was always small for CrII-FeII but remarkable for CrII-FeI, suggesting that the line Fe 2689.21A is blended but appears as it were Fe II line. The influence of the gap distance on the ratio for some line-pairs is shown in Table 1.

Table 1. Influence of the gap distance (d) on the relative intensity of line-pairs.

Group	Line-pair			$\Delta E(eV)^{1)}$	Ir(A)	Ir(B)	Ir(A)/Ir(B)
I	(1)	CrII2677.16	/FeII2730.74	+0.59	0.15_3	0.16_7	0.91
	(2)	〃	/FeII2619.08	+2.52	0.34	0.46	0.75
	(3)	〃	/FeII2630.07	+2.55	0.22	0.29	0.76
	(4)	〃	/FeII2751.12	+2.68	0.52	0.59	0.88
	(5)	〃	/FeII2716.22	+2.97	0.16_3	0.22_7	0.71
	(6)	〃	/FeII2637.64	+3.02	0.39	0.59	0.68
	(7)	〃	/FeII2707.13	+4.04	0.50	0.79	0.64
?	(8)	〃	/Fe 2689.21	?	0.65	0.58	1.12
I'	(9)	〃	/FeI2720.90	−8.31	0.61	0.19	3.20
	(10)	〃	/FeI2733.58	−7.53	0.44	0.19	2.31
	(11)	〃	/FeI2735.48	−7.48	0.64	0.28	2.28
	(12)	〃	/FeI2806.98	−7.59	1.17	0.58	2.02

In Table 1 symbols are as follows:
Group I: In this group the line-pairs are the pairs of CrII line—FeII line.
Group I': In this group the line-pairs are the pairs of CrII line—FeI line.
?: This symbol means that the classification of the line Fe 2689.21A is uncertain.
$\Delta E = E_{Fe} - E_{Cr}$
E_{Fe} = E.P. of Fe spectral line.
E_{Cr} = E.P. of Cr spectral line.
$Ir = (I_{Cr}/I_{Fe})^{\gamma}$, "the relative intensity"
γ: so-called gamma, the contrast factor of emulsion.
Ir(A): Ir in the case of d=1mm
Ir(B): Ir in the case sf d=4mm

III. Discussion

3.1 *Classification of the line* FeI 2689.21A

The line FeI 2689.21A is considered to be classified as

Spectral line	Classification*	E(eV)**
FeI 2689.21A	$a^5F_4 - v^5D_3^0$	5.52

* Designation of the Multiplet depends on reference 3).
** Excitation Potential calculated by the author.

Table 2. Combinations of a^5F and v^5D°

Classification	Wavelength λ_o(A) (observed)[3]	Wavelength λ_c(A) (calculated)[3][4]	$\Delta\lambda=\lambda_o-\lambda_c$	E(eV)
$a^5F_5-v^5D^\circ_4$	2666.818	2666.810	0.008	5.51
$a^5F_4-v^5D^\circ_4$	2699.107	2699.100	0.007	5.51
$a^5F_4-v^5D^\circ_3$	2689.212	2689.207	0.005	5.52
$a^5F_3-v^5D^\circ_4$	2724.959	2724.951	0.008	5.51
$a^5F_3-v^5D^\circ_3$	2714.868	2714.863	0.005	5.52
$a^5F_3-v^5D^\circ_2$	2706.581	2706.580	0.001	5.54
$a^5F_2-v^5D^\circ_3$	2734.004	2734.000	0.004	5.52
$a^5F_2-v^5D^\circ_2$	2725.606	2725.599	0.007	5.54
$a^5F_2-v^5D^\circ_1$	2718.435	2718.435	0	5.55
$a^5F_1-v^5D^\circ_2$	2738.213	2738.212	0.001	5.54
$a^5F_1-v^5D^\circ_1$	2730.984	2730.981	0.003	5.55
$a^5F_1-v^5D^\circ_0$	2726.054	2726.056	0.002	5.56

Note: E=Excitation Potential

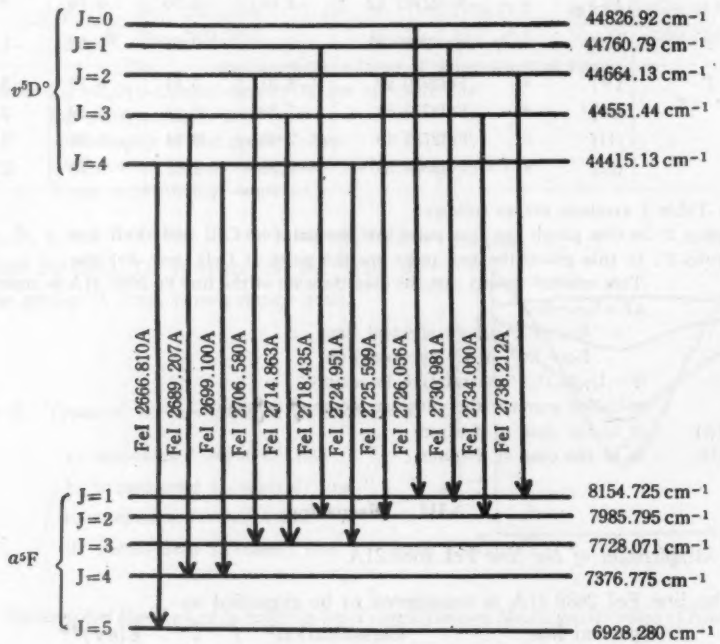

Fig. 4 Schematic interpretation of the combinations $a^5F-v^5D^\circ$

3) C. E. Moore: Atomic Energy Levels, Vol. II (1952).
4) H. Kayser: Tabelle der Schwingungszahlen (1925).

All Fe lines which can originate theoretically from the combination $a^5F-v^5D^o$ were observed as shown in Table 2.

In Table 2, the wavelengths calculated from atomic energy levels[3)4)] are in good agreement with the corresponding observed values[2)] which testify the correctness of the classification of the line FeI. Combinations of a^5F and v^5D_o are shown in Fig. 4 for reference.

3.2 *Classification of the line* FeII 2689.21A

This line is reasonably classified as

Spectral line	Classification	E(eV)
FeII 2689.21A	$b^3P_{3/2}-y^4D_{3/2}^o$	15.70

FeII lines which can originate theoretically from the combination b^3P-y^4D were observed as shown in Table 3. Schematic interpretation of term-combination is in Fig. 5.

Table 3. Combinations of b^3P and y^4D^o

Classification	Wavelength λ_o(A) (observed)[2)]	Wavelength λ_c(A) (calculated)[3)4)]	$\Delta\lambda=\lambda_o-\lambda_c$	E(eV)
$b^3P_{3/2}-y^4D_{5/2}^o$	2709.056	2709.052	0.004	15.67
$b^3P_{3/2}-y^4D_{3/2}^o$	2689.212	2689.207	0.005	15.70
$b^3P_{1/2}-y_4D_{3/2}^o$	2774.691	2774.684	0.007	15.70

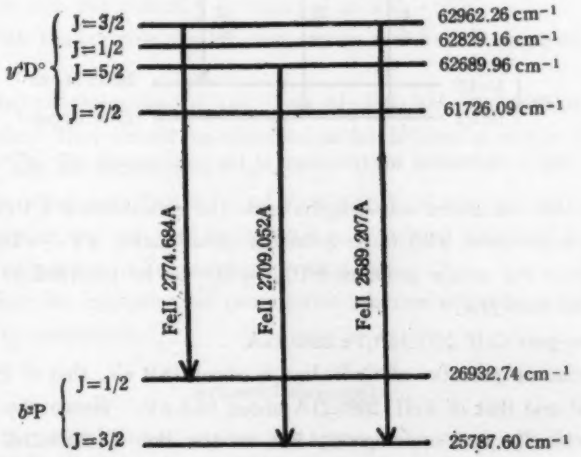

Fig. 5 Schematic interpretation of the combinations $b^3P-y^4D^o$

The configuration of the multiplet y^4D^o is $3d^6$ (a^3P) 4p, and is the same as that of the multiplet z^3D^o. There should naturally be an interaction between

y^4D^o and z^2D^o. $z^2D^o_{5/2}$ and $y^4D^o_{5/2}$ should perturb each other as should also $z^2D^o_{3/2}$ and $y^4D^o_{3/2}$. Therefore, if the intersystem combinations $b^2P-y^4D^o$ occur as seen in Table 3, normal combinations $b^2P-z^2D^o$ must necessarily also occur, and the Fe II lines, which can originate theoretically from the combination $b^2P-z^2D^o$ were in fact observed as given in Table 4. The schematic interpretation of term-combination is shown in Fig. 6.

Table 4. Combinations of b^2P and z^2D^o

Classification	Wavelength λ_o(A) (observed)[3]	Wavelength λ_c(A) (calculated)[5][4]	$\Delta\lambda=\lambda_o-\lambda_c$	E(eV)
$b^2P_{3/2}-z^2D^o_{5/2}$	2831.562	2831.567	0.005	15.47
$b^2P_{3/2}-z^2D^o_{3/2}$	2751.123	2751.124	0.001	15.60
$b^2P_{1/2}-z^2D^o_{3/2}$	2840.647	2840.647	0	.15.60

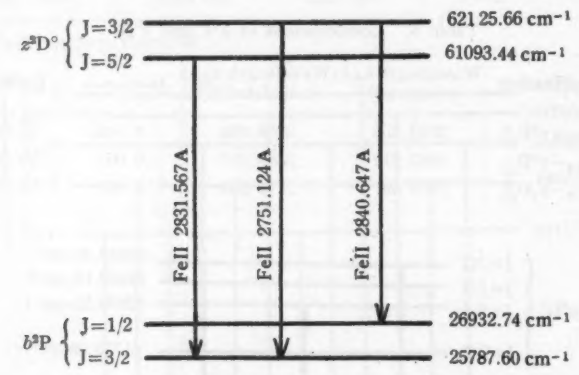

Fig. 6 Schematic interpretation of the combinations $b^2P-z^2D^o$

Further, the calculated wavelengths from the classification $b^2P_{3/2}-y^4D^o_{3/2}$ are in complete argreement with those from the classification $a^5F_4-v^5D_3^\circ$ (Tables 2 and 3), whence the author proposes $b^2P_{3/2}-y^4D^o_{3/2}$ to be recorded as the classification of FeII 2689.21A.[5]

3.3 *The line-pair* CrII 2677.16A/Fe 2689.21A

The excitation potential of Cr II line is about 12.9 eV, that of FeI 2689.21A about 5.5 eV and that of FeII 2689.21A about 15.7 eV. Hence the line-pair Cr II/FeI is evidently not homologous. But as the line Fe 2689.21A is blended-its FeII component being predominant in Feussner spark excitation, the line-pair CrII 2677.16A/Fe 2689.21A may appear as though homologous.

5) Letter from Dr. C. E. Moore (June, 1956)

3.4 *Some Mn spectral lines*

Classifications of the lines Mn 2939.30A and 2933.06A are not given in M.I.T. wavelength tables. But, the present experiments have given good reason to classify them as Mn II lines as shown in Table 5[1)6)7)] which tells that the line-pairs Mn 2939.30A/FeII 2926.59A and Mn 2933.06A/FeII 2926.59A are both homologous* and are expected to be stable and suitable for quantitative spectrochemical analysis of Mn in steel. It is natural that, from mere experience, these line-pairs have been in use with satisfactory results.

Table 5 Classifications of Some Mn Spectral Lines

Spectal line	Classfication	E(eV)
Mn 2939.30A	$a^5S_2-z^5P^o_2$	12.82
Mn 2933.06A	$a^5S_2-z^5P^o_1$	12.83

IV. Conclusion

The following conclusions are drawn from the results.

(1) In Feussner spark excitation, the intensity of spectral lines along their paths between electrodes has four types of distribution as shown by a, b, c and d in Fig. 3.

(2) The usual classification of the line Fe 2689.21A as FeI is not correct. This line is a blend of FeI and FeII lines.

(3) The line FeI 2689.21A is classified as $a^5F_4-v^5D^o_3$.

(4) With reason, the classification of the line FeII is proposed as $b^2P_{3/2}-y^4D^o_{3/2}$.

(5) The classifications of the lines Mn 2939.30A and 2933.06A have not yet been made. They should be classified as Mn II lines in which Mn 2939.30A as $a^5S_2-z^5P^o_2$ and Mn 2933.06A as $a^5S_2-z^5P^o_1$.

(6) The line-pair CrII 2677.16A/Fe 2689.21A is not an exceptional pair but is homologous, for the line Fe 2689.21A is a blended line and its FeII component is predominant in Feussner spark excitation.

(7) That the line-pairs for quantitative spectrochemical analysis should be homologous is ascertained.

Acknowledgements

The author would like to express his appreciation to Dr. H. Hasunuma, Dr. M. Kamiyama and Dr. C. E. Moore for their kind encouragement and suggestion.

6) C. W. Curtis: Phys. Rev. **53** (1938) 474.
7) C. E. Moore: Ultraviolet Multiplet Table, N.B.S. Circ. 488 (1952)
* Excitation Potential of FeII 2926.59A is 13.12 eV.

Optical Properties of Some Metallo-Organic Salts of 8-Hydroxyquinoline

Sumitada ASANO

Department of Physics, Faculty of Science, Okayama University

and

Yasuharu NISHIKAWA

Department of Chemistry, Faculty of Science, Okayama University

(Received March 8, 1956)

Abstract

Luminescent properties and spectral reflectances of some metallo-organic salts of 8-Hydroxyquinoline are investigated at a room temperature. As metallic elements alkali-earth metals, Zn, Cd and earth metals are used. The peak wave-lengths of their luminescences under UV excitation lie within the range 490···540 mμ, and in efficiently luminescent salts a strong absorption band is observed near 400 mμ regardless of the kind of metallic element. According to the results obtained, the metal ions in these salts seem to have no direct concern in luminescence process.

1. Introduction

8-Hydroxyquinoline (abbreviated as oxine) has been used widely as precipitant for qualitative and quantitative analyses of various metal ions. It is well-known that some of these metallo-organic salts of oxine (abbreviated as oxinates) can show luminescence in crystalline state as well as in solution state dissolved in some organic solvents such as chloroform and alcohol. Hitherto the luminescent properties and absorption spectra of various oxinates dissolved in organic solvents have often been investigated with a view to apply these optical properties to quantitative analysis[1].

This paper deals with the results of the investigations on the luminescent properties and spectral reflectances of the crystalline oxinates of alkali-earth metals, Zn, Cd and earth metals at a room temperature.

1) T. Moeller: Ind. Eng. Chem. Anal. Ed. **15** (1943) 270, 346.
T. Moeller and A. J. Cohen: ibid. **22** (1950) 686.
H. Goto: J. Chem. Soc. Japan **59** (1937) 547, 625.
E. Goon, J. E. Petley, W. H. McMullen and S. E. Wiberly: Anal. Chem. **25** (1953) 608.
E. B. Sandell: Ind. Eng. Chem. Anal. Ed. **19** (1947) 63.

2. Preparation of Samples

To a solution containing about 20 mg of metal ions were added 15–20 ml of 2%-Oxine-1N-acetic acid solution and 20 ml of 20%-ammonium acetate buffer solution. After having made the total volume equal to about 100 ml by adding water, the pH of the solution was adjusted to the optimum value (cf. Table I)

Table I

Sample Notation	Metal Ion	Applied pH Value	Drying Temperature (°C)	Chemical Formula*	Relative Peak Output (3650 Å Excitation)
BeA	Be^{2+}	9.4	110	$BeO(Ox)_2 2H_2O$	11
BeB	〃	〃	130	···	24
MgA	Mg^{2+}	9.5	105	$Mg(Ox)_2 2H_2O$	9
MgB	〃	〃	140	$Mg(Ox)_2$	13
Ca	Ca^{2+}	9.7	105	···	7
Sr	Sr^{2+}	10.0	65	···	1
Ba	Ba^{2+}	8.4	20	···	···
ZnA	Zn^{2+}	4.7	105	$Zn(Ox)_2 3/2H_2O$	68
ZnB	〃	〃	130	$Zn(Ox)_2$	46
CdA	Cd^{2+}	9.7	105	$Cd(Ox)_2 3/2H_2O$	10
CdB	〃	〃	140	$Cd(Ox)_2$	11
Al	Al^{3+}	4.8	105	$Al(Ox)_3$	57
Ga	Ga^{3+}	4.1	110	$Ga(Ox)_3$	19
In	In^{3+}	6.0	105	$In(Ox)_3$	8
Tl	Tl^{3+}	5.0	110	$Tl(Ox)_3H_2O$	···

* $(Ox) = (C_9H_6ON)$

by using NH_4OH in order to precipitate the metal ions completely. The precipitate thus obtained was digested on a water-bath at 70°C for about 20 minutes and allowed to stand for 1–2 hours. Then the precipitate on the bottom of the vessel was separated by a glass-filter and washed with water sufficiently so that excess oxine might be thoroughly removed. The crystalline oxinate was finally obtained by drying the separated precipitate for 2–3 hours at the temperature shown in Table I[2]. The fifth column of Table I indicates the chemical formulae which have been determined by chemical analysis[3].

The oxine reagent used in the above procedures had been purified by steam distillation.

2) L. L. Merrit. Anal Chem. **25** (1953) 719.
3) S. Ishimaru: J. Chem. Soc. Japan **53** (1932) 566.
W. Geilmann and F. W. Wrigge: Z. Anorg. Chem. **209** (1932) 129.
T. Moeller and A. J. Cohen: loc. cit.
K. Motojima: J. Chem. Soc. Japan **77** (1956) 95.

3. Luminescent Properties

The spectral-distribution curves of the luminescences of the prepared oxinates under UV excitation are shown in Fig. 1 a–c. The luminescent emission was

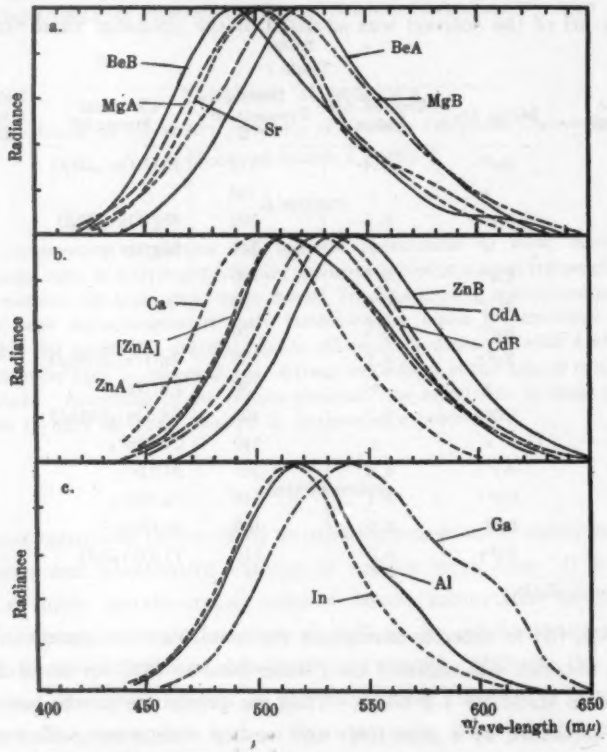

Fig. 1 Spectral-distribution curves of luminescences of the oxinates prepared. All the curves were measured under 3650 Å excitation except the curve [ZnA] in diagram b, which was obtained under 2537 Å excitation.

picked up by a Mazda multiplier tube (MS-9S). The details of the measuring apparatus are given in the previous paper[4]. The sample was a thick layer which was obtained by spreading the wet precipitate of an oxinate uniformly on a glass-plate and drying it at the temperature shown in Table I.

Although the peak wave-length varies with the kind of metal ion or by

4) S. Asano: Sci. of Light (Tokyo), **4** (1955) 32.

hydration, it lies within the comparatively narrow range 490–540 mμ, as shown in Fig. 1. The peak wave-lengths in oxinates of alkali-earth metals tend to be somewhat shorter than those of oxinates of earth metals, Zn and Cd. The relative peak output under constant 3650 Å excitation is shown in the last column of Table I. All the salts which were luminescent under 3650 Å excitation (Mazda SHL-100+Mazda UVD-2 Filter) were also luminescent under 2537 Å excitation (Mazda Germicidal Lamp+Corning 9863 Filter). According to the experimental results, the distribution curve under 2537 Å excitation is thoroughly similar to that under 3650 Å excitation in one particular salt, as exemplified in Fig. 1b. Among the oxinates prepared, Sr salt showed only weak luminescence, and Ba and Tl salts were non-luminescent.

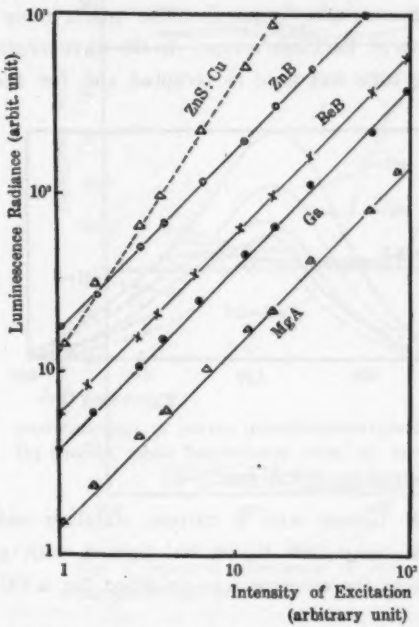

Fig. 2 Dependence of luminescence output upon intensity of excitation. Excited by 3650 Å line.

Fig. 2 shows the dependence of the luminescence output upon the intensity of excitation. Since it had been previously assured that the shape of spectral-distribution curve is almost independent of the in tensity of excitation in one particular salt, the relative output was measured at the peak wave-length. The sample was excited at various distances from the excitant source and the relative intensities of excitation incident upon the sample were measured by a photo-tube (Mazda PSV-50Y) connected to a DC amplifier[5]. In addition, the result obtained with a hex-ZnS:Cu phosphor is shown in the same figure. It should be noted that the dependence of the luminescence output I upon the intensity of excitation J is nearly linear in all the luminescent oxinates, whereas I varies as J^n $(n>1)$ in the ZnS phosphor[6].

Further, the salts of the same metal ion were prepared under various pH values and then the spectral-distribution curves of their luminescences under the

5) L. A. Dubridge and H. Brown: Rev. Scient. Instr. **4** (1933) 532.
6) G. F. J. Garlick and A. F. Gibson: J. Opt. Soc. Am. **39** (1949) 935.

same given conditions were compared with one another. These curves were quite similar in shape, as exemplified in Fig. 3. The heights of the curves in Fig. 3 are plotted relatively to their own radiances.

4. Spectral Reflectance

Reflection spectra of some of the salts prepared were measured by the apparatus similar to that devised by Botden and Kroger [7]. The quartz monochromator used for the measurements was of Beckman's type. In the wave-length range shorter than 440 mμ a RCA 1P28 tube was used as receptor and for the range longer than that wave-length a RCA 1P22 tube. In the former range a glass filter (Mazda V-Y2C. Cut-off wave-length: 440 mμ) was used in order to separate the excited luminescent emission from the monochromatic UV or violet ray reflected on the sample surface. The UV source was a hydrogen discharge tube (Shimadzu. 80V. 300 mA) lighted with a current stabilizer and the visible source was an incandescent lamp (100 V. 40 W.) lighted with a voltage stabilizer. The photo-current from the receptor was amplified by a DC amplifier[8].

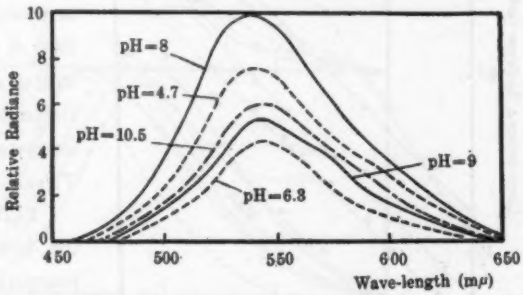

Fig. 3 Spectral-distribution curves of luminescences of anhydrous Zn salts precipitated under various pH values. Excited by 3650 Å line.

Pure MgO powder (Merk's guaranteed reagent) was used as the standard of reflectance. The sample was of a thick layer (about 1 mm in thickness) stuffed mechanically (without binder) in a shallow rectangular tray (10×25 mm^2) of thin metal sheet.

The results obtained are shown in Fig. 4a—c. The fact that two spectral-reflectance curves of one particular salt, which were measured in the two wave-length ranges, connect with each other continuously at about 450 mμ even in the cases of the luminescent salts, shows that the emissions excited by the visible rays at the wave-lengths longer than 450 mμ are quite negligible. The

7) Jh. P. J. Botden and F. A. Kröger: Physica **15** (1949) 747.
8) K. L. McDonald and F. S. Harris: J. Opt. Soc. Am. **42** (1952) 321.
T. Namioka: Sci of Light (Tokyo) **3** (1954) 15.

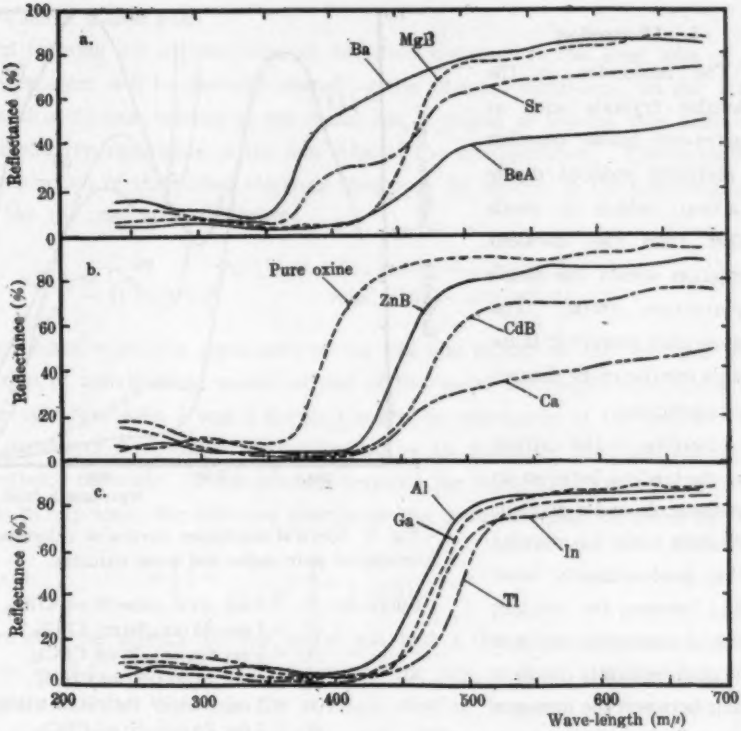

Fig. 4 Spectral reflectances of pure oxine and some oxinates, relative to a standard MgO powder.

spectral reflectances of most of the oxinates prepared (Mg, Zn, Cd and earth metal salts), which have yellow reflection color under day-light, have similar features. They have very low reflectance in the range shorter than about 450 mμ, and beyond this wave-length their reflectances rise rapidly towards longer wave-lengths to reach to nearly constant values. These results are in good agreement with the absorption curves in Fig. 5, obtained with chloroform solutions of these oxinates. In the case of Sr and Ba salts which have pale-yellow reflection color, the threshold wave-length nearly coincides with that of pure oxine (about 360 mμ) and the reflectance has the trend to increase gradually towards longer wave-lengths. The curves of Be and Ca salts have similar features to each other. These salts have a darkish-yellow reflection color.

5. Discussion

The molecules in the molecular crystals such as oxinates are bound together by mutually induced dipole attraction, which is much weaker than the covalent interaction within the single ring-structure units. The luminescence centers in these crystals are therefore distinct single molecules.

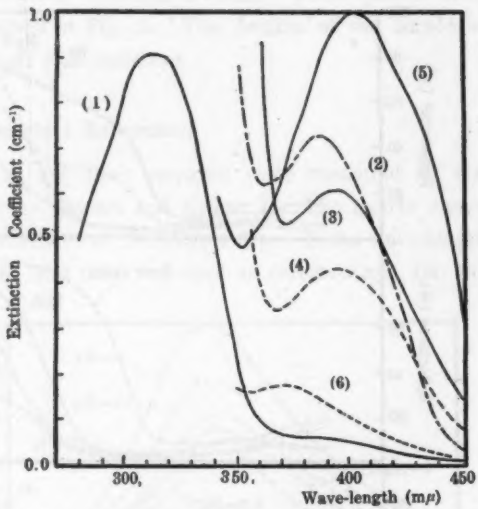

Fig. 5 Spectral-absorption curves of chloroform solutions of pure oxine and some oxinates.

Curve no. (1) 5.6 mg pure oxine/50 ml $CHCl_3$
(2) 5.1 mg Al $(ox)_3$/50 ml $CHCl_3$
(3) 0.5 mg Ga $(ox)_3$/50 ml $CHCl_3$
(4) 1.4 mg In $(ox)_3$/50 ml $CHCl_3$
(5) 0.3 mg Tl $(ox)^3$ H_2O/50 ml $CHCl_3$
(6) 2.7 mg Zn $(ox)_2$/50 ml $CHCl_3$

According to the current view, the binding between an oxine molecule and a divalent or trivalent metal ion consists of the predominantly ionic binding between the oxygen atom and the metal ion and of the predominantly covalent binding between the nitrogen atom and the same metal ion. (cf. Fig. 6) In the nitrogen atom of an isolated oxine molecule, two of the three $2p$-orbitals are hybridized with the $2s$-orbital and they form three s^1p^2 lobe-like orbitals extending equiangularly in the plane of the aromatic rings, whereas the remaining $2p$-orbital jutting out perpendicularly to the plane of the aromatic rings makes a molecular orbital together with those of the π-electrons of other carbon atoms[9]. An electron in each one of the two lobes pointing towards the two adjacent carbon atoms makes a covalent bond with each one of them res-

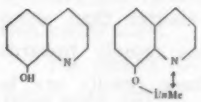

Fig. 6 Structural formulae of an an oxine molecule (*left*) and one co-ordinated group in an oxinate molecule (*right*).

Me: Metal ion
$n=2$ for divalent alkali-earth metal ions, Zn^{2+} and Cd^{2+}.
$n=3$ for trivalent earth metal ions.

9) H. J. Emeléus and J. S. Anderson: *Modern Aspects of Inorganic Chemistry* (D. Van Nostrand Co. N.Y. 1952) p 147.

pectively, and the remaining lobe is filled with two electrons of opposite spins which make a lone pair.

In forming an oxinate, one of the two electrons in the lone lobe of the nitrogen atom will be partially shared by the adjacent metal ion. In the state, when this electron belongs to the metal ion, it makes a bonded pair with the other electron remaining in the lone lobe of the nitrogen atom. The normalized wave-function of the paired electrons then may be written in the following form just like the case of zincblende[10]:

$$\varphi(1,2)=\frac{1}{[1+2A^2]^{1/2}}\{u(1)u(2)+A[u(1)v(2)+u(2)v(1)]\}\times[\alpha(1)\beta(2)-\alpha(2)\beta(1)]/\sqrt{2} \qquad (5.1)$$

where u and v are the space part of the lobe-like orbital of the nitrogen atom and that of a hybridized valence-orbital of the metal ion respectively, and α and β the spin functions. 1 and 2 denote the sets of coordinates of the two electrons. The parameter A should be determined so as to minimize the total energy of the oxinate molecule. If the binding between the oxygen atom and the metal ion is purely ionic, the effective charge on the metal ion may be given by[10].

$$ne\left[1-\frac{2A^2}{1+2A^2}\right]=\frac{ne}{1+2A^2}\ , \qquad (5.2)$$

where n is the valency of the metal ion and e the electronic charge. When $A=\infty$ in (5.1), the ionic binding between the oxygen atom and the metal ion therefore vanishes, although the covalent binding between the nitrogen atom and the metal ion becomes tight instead. When $A=0$ in (5.1), the covalent bond does not exist. Accordingly in a stable oxinate molecule A would be expected to take a comparatively large finite value.

As a measure of the affinity of the metal ion for the fluctuating electron its polarizing power p (ratio of ionic valency to ionic radius) may be used[11]. For a metal ion having a comparatively large p value, A will take a non-zero value. The larger the value of p of a metal ion is, the larger the value of A minimizing the energy will be. The values of p of the metal ions used in the experiments are shown in Table II.

According to the experimental results, the metal ions having relatively large p values (>2), in general, make stable salts with oxine, and these salts except Tl salt are efficiently luminescent. As easily infered from Fig. 4a, the

10) S. Asano and Y. Tomishima: J. Phys. Soc. Japan **11** (1956) 644

11) H. W. Leverentz: *Introduction to Luminescence of Solids.* (John-Wiley & Sons Co. N.Y. 1950) p 410.

Table II

Metal Ion	Ionic Radius (Å)*	Value of p	Metal Ion	Ionic Radius (Å)*	Value of p
Be^{2+}	0.31	6.45	Zn^{2+}	0.47	2.70
Mg^{2+}	0.65	3.08	Cd^{2+}	0.97	2.06
Ca^{2+}	0.99	2.02	Al^{3+}	0.50	6.00
Sr^{2+}	1.13	1.77	Ga^{3+}	0.62	4.48
Ba^{2+}	1.35	1.48	In^{3+}	0.81	3.70
			Tl^{3+}	0.95	3.16

* Pauling's computed value

precipitates formed in the solutions of Sr^{2+} and Ba^{2+}, which have relatively small p values (<2), tend to decompose, to a great extent, in drying them, and a large quantity of oxine has been isolated in the dried solids. This is actually evidenced also by the facts that these samples conspicuously gave out the smell of oxine in drying process, and that Sr salt showed only weak luminescence and Ba salt was non-luminescent. (cf. Table I).

This rule however is not always valid. For example, Cd salt is more stable than Ca salt and the former is more efficiently luminescent than the latter, although the p value of Cd^{2+} is nearly comparable to that of Ca^{2+}. According to experiments, Ca salt tends to somewhat blacken under prolonged UV irradiation and its luminescence efficiency falls gradually. The fact that Zn^{2+} and Cd^{2+} have larger electron affinities to form covalent bonds with the atoms adjoining them than those of alkali-earth metal ions, is recognized also in sulphides and selenides of these metals[10].

As shown in Fig. 3, the pH value in precipitating an oxinate does not affect the state of binding in any essential way, except that the precipitation is restrained, to some extent, or not realized under a low pH value.

As shown in Figs. 4 and 5, a strong absorption band appears at about 400 mμ, regardless of the kind of metal ion, when the binding between the oxine molecule and the metal ion is comparatively tight. From this fact as well as the fact that the peak wave-length of the emission band shows no wide change with the kind of metal ion (cf Fig. 1), it is inferred that the metal ions in the oxinates would not be concerned directly in luminescence process. The π-electrons on the aromatic rings are subjected to a strong perturbation owing to tight binding between the nitrogen atom and the metal ion, and the luminescence would be ascribable to a new emission level resulting from a spin interaction of these π-electrons. It should be noted that this emission band may be excited effectively also by 2537 Å line which is considerably shorter than the absorption

edge.

Since the luminescence mechanism in the oxinates may be assumed to be of simple monomolecular type on account of the inferences mentioned above, the luminescence output in the stationary state is proportional to $P\eta NS/(P+S)$, where P is the sum of the normal light emission probability ($\approx 10^8$ sec^{-1}) and the non-radiative transition probability, S the excitation probability which is proportional to the intensity of excitation, η the quantum efficiency of luminescence and N the total number of oxinate molecules. For the ordinary intensity of excitation S would be much smaller than P. The luminescence output then depends linearly upon the intensity of excitation in agreement with the results obtained experimentally (cf. Fig. 2). In the case of T1 salt, the energy in the emission level would be dissipated probably by a non-radiative process ($\eta \fallingdotseq 0$), although the binding of Tl^{3+} with oxine is comparatively tight (cf. Fig. 4c).

In closing, the authors express their sincere thanks to Dr. Y. Uehara of the Mazda Laboratory (Tokyo-Shibaura Elc. Co.) for helpfull advice and to Mr. Y. Tomishima for valuable discussion in performing this work.

On the Near Ultra-violet Absorption Spectra of Tropolone Derivatives

(I) Gaseous Hinokitiol and α-Thujaplicin

Kwan-ichi ASAGOE and Yoshiro OKISHIMA

Department of Physics, Faculty of Science, Okayama University

(Received May 13, 1956)

Abstract

Ultra-violet absorption spectra of hinokitiol and α-thujaplicin, both in gaseous states and as water solutions, are obtained in the region 2300–4000 Å. Comparisons of the spectra are made first for the two compounds in gaseous states, then for α-thujaplicin and tropolone as water solutions. Further vibrational analysis in detail was restrained because of their diffuse nature.

1. Introduction

Absorption spectra of tropolone and some of its derivatives in infra-red and ultra-violet regions were investigated by Dr. Nozoe, Professor of the Tohoku University, and his collaborators[1]. Their investigations were made with specimens dissolved in solvents and there are yet no data available for their gaseous states. On the other hand, the studies on benzene and its derivatives[2][3] show that the absorption spectra of the vapours reveal more detailed structure than those of the liquid samples and it had been able to decide accurately the molecular vibrational structure in both normal and excited states. Hence, with the intention of investigating the near ultra-violet absorption spectra of tropolone derivatives especially in gaseous state, this experiment was carried out.

Fortunately, in Prof. Yamane's laboratory (Faculty of Science, Okayama University) various kinds of the tropolone derivatives had been synthesized, and samples were kindly offered to the authors. The investigation of the near ultra-violet absorption spectra of hinokitiol and α-thujaplicin was thus undertaken in the first place.

Various resonance structures of tropolone have been proposed by a number

1) T. Nozoe, T. Mukai, M. Kinori: Methyltropolone and its Derivatives. (Published by the Faculty of Science, Tohoku Univ., Jan. 1952).

2) Kistiakowsky: Journ. Chem. Phys. **5** (1937), 609.

3) K. Asagoe and his coworkers: Proc. Phys.-Math. Soc. Japan **22** (1940), 677; 685, etc.

of workers[1)4)]. Dr. Nozoe assumed that tropolone might be a resonance hybrid of (a), (b) and (c) types shown below.

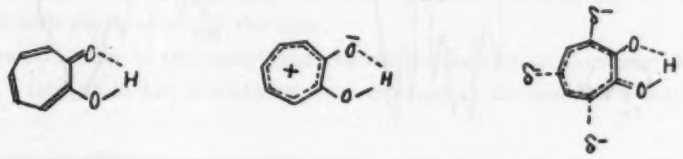

(a) (b) (c)

The results of measurements on various characteristics, i.e the dipolemoment, the infra-red and Raman spectra, etc. pointed out a high probability of the presence of a structure such as (b) in its normal state, that is, tropolone nucleus is charged positively owing to the migration of an electron to O-atom, the remaining six electrons being able to circulate in a ring.

Several absorption spectra of tropolone and its derivatives which were previously investigated[1)] are reproduced in Figs. 1, 2 and 3, two of which have a close similarity, notwithstanding the different substituent, and this appears to indicate that the absorption characters are mainly due to the tropolone nucleus.

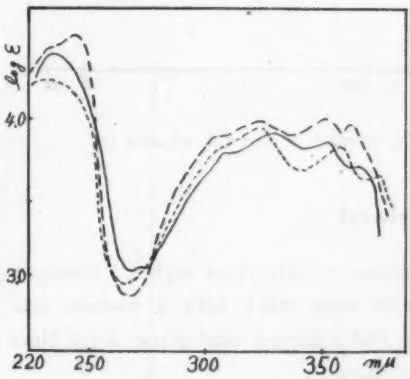

Fig. 1. Ultra-violet absorption spectra in cyclohexanone
1) *o*-methyltropolone (- - - -)
2) *m*-methyltropolone (——)
3) *p*-methyltropolone (·····)

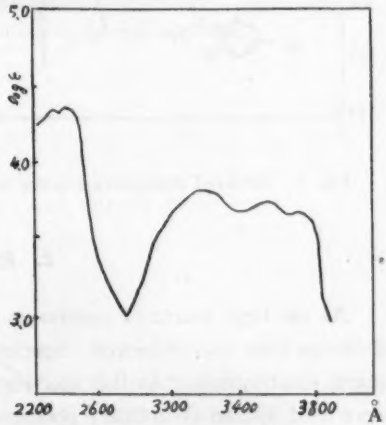

Fig. 2. Ultra-violet absorption spectrum of tropolone in ethanol.

4) J. W. Cook, A. R. Gibb, R. A. Raphael and A. R. Somervilie: Journ. Chem. Soc. (1951), 503

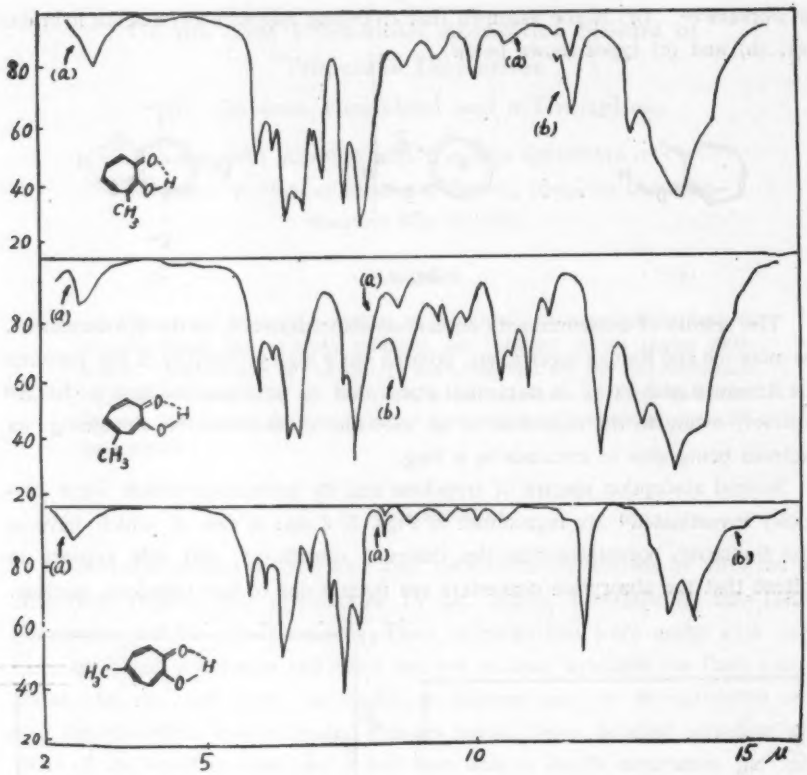

Fig. 3. Infra-red absorption spectra in CCl_4 solution (a) and CS_2 solution (b)

2. Experiment

As the light source of continuous spectrum in ultra-violet region, a hydrogen discharge tube was employed. Spectrograms were taken with a medium size quartz spectrograph. As this spectrograph had a curved focal plane, X-ray films were used instead of ordinary photographic plates.

The absorption tube was made using a pyrex glass tube of 16 mm in diameter of a suitable length for each sample, both ends of which were provided with fused silica windows. After the sample had been put in its side tube, the tube was evacuated and sealed. Then the tube was filled with the vapour under the proper pressure corresponding to the temperature of the sample.

While hinokitiol was being examined, the side tube containing the sample

was cooled by a mixture of solid and liquid benzene or ice water because of its high vapour pressure at a room temperature. In the case of α-thujaplicin, the tube was put in a tank filled with hot water (68°C). The tank had two windows aligned with the windows of the tube.

Next, in order to photograph the absorption spectrum of the water solution, a Baly's tube of 19 mm in diameter was employed as the absorption bath.

3. Hinokitiol

Hinokitiol (β-thujaplicin), discovered by Dr. Nozoe, is the tropolone derivative by the substitution of an isopropyl-group. The structure is acknowledged as shown in the following.

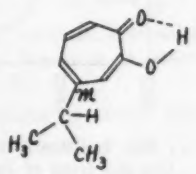

Its melting point is 52°C, and the boiling point is 140°C at 10 mmHg.

(A) The absorption spectrum of gaseous hinokitiol.

In this experiment, an absorption tube of 260 mm in

Fig. 4. Ultra-violet absorption spectrum of gaseous hinokitiol.

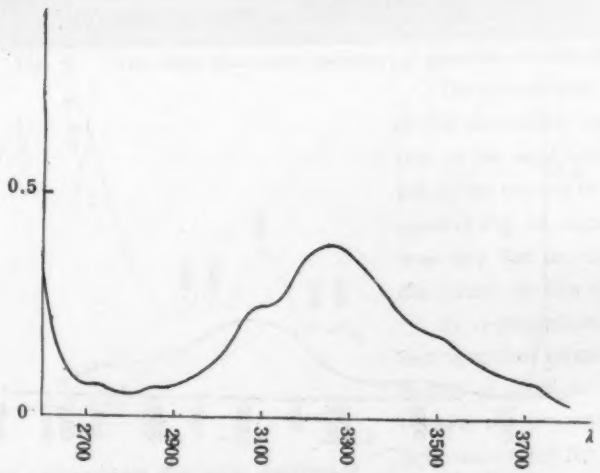

Fig. 5. Ultra-violet absorption spectrum of gaseous hinokitiol (2700–3700 Å)

length was used. The absorption spectrum of the region longer than 2700 Å could be obtained by cooling the side tube with the mixture of solid and liquid benzene (about 6°C) and the spectrum between 2300 and 2700 Å by ice water.

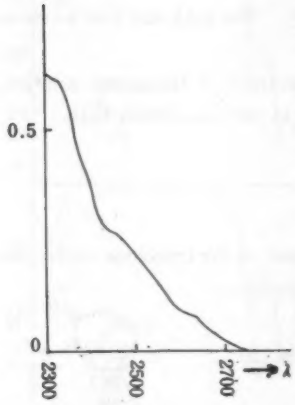

Fig. 6. Ultra-violet absorption spectrum of gaseous hinokitiol (2300–2700 Å)

The spectrum thus obtained is shown in Fig. 4. In order to determine the intensity distribution of the absorption bands, the blackness curves of the absorption spectrum and continuous spectrum of hydrogen discharge were registered with a microphotometer respectively and relative ratio of the two curves was calculated at corresponding regions of the spectra. The graphs thus plotted are shown in Figs. 5, 6. (ordinates of the graphs are in arbitrary unit.) The wave lengths of the absorption bands were determined by comparing with an iron spectrum photographed on the same film of the absorption spectra.

(B) The absorption spectrum of hinokitiol dissolved in water.

The absorption spectrum beyond 2700 Å of water solution of hinokitiol was

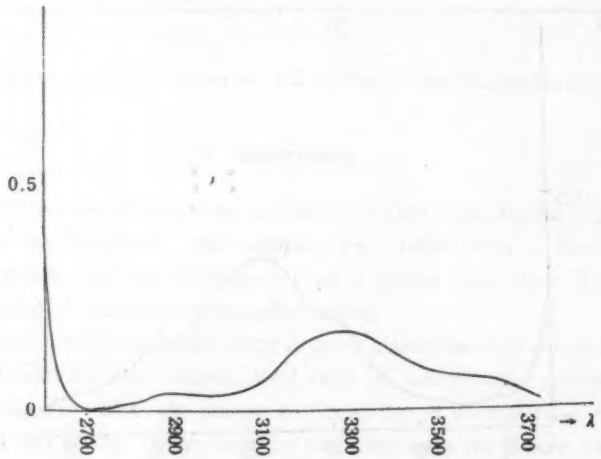

Fig. 7. Ultra-violet absorption spectrum of hinokitiol in water (2700–3700 Å).

photographed by using a Baly's tube of 70 mm in length, and that between 2300 and 2700 Å by the tube length of 10 mm. The curves showing the intensity ratios are given in Figs. 7, 8.

4. α-thujaplicin

α-thujaplicin is a tropolone derivative by the substitution of an isopropyl-group at an ortho-position of tropolone nucleus.

There are two states of crystal; one is of m.p. 25°C, the other is of 34°C. The latter sample was investigated in this experiment.

(A) The absorption spectrum of gaseous α-thujaplicin.

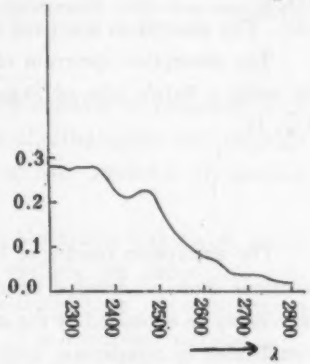

Fig. 8. Ultra-violet absorption spectrum of hinokitiol in water (2300–2700 Å).

Considering the facts that the melting point of α-thujaplicin is lower than that of hinokitiol by about 20°C and the absorption power of hinokitiol was very strong as seen in the previous experiment, α-thujaplicin is reasonably expected to show still stronger absorption power. Hence, an absorption tube of 170 mm in length which is 90 mm shorter than the previous one was first employed. The absorption spectrum, however, could not be obtained at a room temperature and that of suitable intensity was obtained at a rather higher temperature of 68°C. The results thus obtained are shown in Figs. 9, 10.

Fig. 9. Ultra-violet absorption spectrum of gaseous α-thujaplicin.

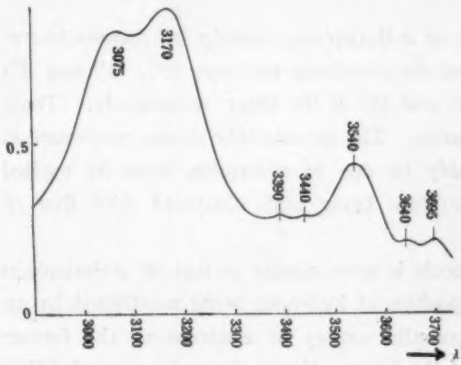

Fig. 10. Ultra-violet absorption spectrum of gaseous α-thujaplicin.

The comparison of the curve of the absorption spectrum with that of the light source was omitted in the process of obtaining the curve of Fig. 10, because the latter was very flat as compared with the former in this case.

In α-thujaplicin, the absorption spectrum ranging from 2300 to 2700 Å could not be observed because of low intensity of the light source and the diffuse nature of the absorption spectrum in this

region.

(B) The absorption spectrum of α-thujaplicin dissolved in water.

The absorption spectrum of water solution of α-thujaplicin was photographed by using a Baly's tube of 70 mm in length. The result obtained is shown in Fig. 11.

5. Discussions

The absorption spectra of both compounds in gaseous states and as water solutions show no detailed structure against the authors' speculation. This may reasonably be explained by the structure of tropolone nucleus which is remarkably complicated in comparison with that of benzene and has no symmetry property.

(A) The vapour spectra.

In the first place, the absorption spectrum of gaseous α-thujaplicin is compared with that of hinokitiol (Figs. 5, 6 and 10).

The wave lengths of the main absorption maxima of hinokitiol are 3250(a), 3110(b), 3500(c) and 3710(d) in the order of intensity. On the other hand, those of α-thujaplicin are in the order of 3170(a'), 3075(b'), 3540(c'), 3390 (d'), 3440(e') and 3695(f'), (d') and (e') being small maxima.

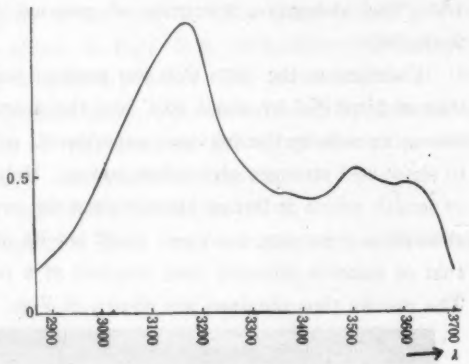

Fig. 11. Ultra-violet absorption spectrum of α-thujaplicin in water.

The highest intensity maximum of α-thujaplicin, namely (a'), seems to correspond to that of hinokitiol (a), and the remaining maxima, (b'), (e') and (f') of the former correspond to (b), (c) and (d) of the latter respectively. Those two spectra thus have a close similarity. The considerably strong maximum at 3540(c') of α-thujaplicin may probably be due to absorption from its excited vibrational state owing to the temperature being high compared with that of hinokitiol.

The structure of hinokitiol molecule is quite similar to that of α-thujaplicin with the exception of the different position of hydrogen being substituted by an isopropyl-group, and the values of potential energy of electrons of the former seem slightly to differ from those of the latter. Hence, it may be concluded that the two spectra exhibit very similar appearances with a wholesale shift one over

the other. The spectroscopic evidence is in good agreement with this consideration.

(B) The solution spectra.

Secondly, the spectrum of α-thujaplicin in water solution is compared with that of tropolone (Fig. 2). For the vapour, spectra of α-thujaplicin and tropolone cannot be compared with each other as there are no data available on gaseous tropolone.

As shown in Fig. 2, the wave lengths of main absorption maxima of tropolone dissolved in ethanol given by the previous workers are about 3200(a′), 3500(b′) and 3700(c′). On the other hand, the authors' data on α-thujaplicin are about 3200(a^3), 3500(b^3) and 3610(c^3) (Fig. 11). The absorption maxima (a′), (b′) and (c′) seem to correspond to (a^3), (b^3) and (c^3), respectively. Both spectra thus have quite similar appearances.

As has been previously mentioned, α-thujaplicin is the tropolone derivative by the substitution of an isopropyl-group. The energy levels of tropolone nucleus of α-thujaplicin are probably shifted against those of tropolone under the influence of the substituent, and hence band heads of both spectra are expected to be shifted one over the other as evidenced by the observation.

It was not possible to further the analysis of these diffuse spectra.

Acknowledgement

The writers wish to thank Prof. K. Yamane for the gift of the pure samples.

LETTERS TO THE EDITOR

Photon Periodicity

Lev Akobjanoff.

Inst. Engin. Research, Univ. of California, Berkeley

(Received July 17, 1956)

I. Available Experimental Evidence-PHOTON-KINETICS.

Investigating the nature of radiant energy we have been able to penetrate within the boundaries of photon-wavelength[1]. The more intimate picture of light-particles thus gained yields firstly a confirmation of the individuality of photons, and secondly discloses that they are active only intermittently on reaching some particular condition, which seems to affect them periodically with a frequency inversely proportional to their wavelength.

At a sub-λ scale the beam of light appears dotted, the dots marking the spots where the photons reach their reactive state. These states seem to be attributes of individual photons, and as such independent of the number and the kind of other photons in the beam the overall effect of this periodic recurrence functions like a one-dimensional concentration of activity along the trajectory of photon-flight.

This picture results from a kinetic investigation of the most precisely known reactions of light: absoption, scattering, refraction, (reflection), and the rotation of polarised light.

(1) The law of Bouguier-Lambert-Beer: $I=I_0 \cdot e^{-acd}$, kinetically of the same shape as the law for radioactive decay: $I=I_0 \cdot e^{-\alpha t}$, leads to the conclusion that light-absorption is of the first order *with respect to the absorbent* (its mass, concentration, time of action$\cdots$). This seems to be possible only if photons are partly inactive.

(2) The complex effects of extinction have been artificially decomposed by us into absorption and scattering, using for this black and white suspensions. Black absorption can be calculated precisely using equations:

$$-\frac{dA}{d\lambda}=0; \quad -\frac{dA}{d\lambda}=Q_1(1/\lambda); \quad -\frac{dA}{d\lambda}=Q_2(1/\lambda)^2; \quad -\frac{dA}{d\lambda}=Q_3(1/\lambda)^2+Q_4(1/\lambda)^3,$$

which are kinetically, *with respect to the wavelength*, of the zeroth, first, second, third orders, $(1/\lambda)$ being substituted for concentrations of reactants. This seems to indicate a regularly discontinuous occurrence of reactivity in photons with frequencies inversely proportional to the wavelength.

(3) White scattering shows the same regularities as black absorption and can be described by the same equations. This points out an additional periodicity in photons, which is also a function of $1/\lambda$, of the same frequency as photon-reactivity. Very likely this is a periodicity of the photon mass, assuming that scattering can operate only on the latter.

(4) Refraction-dispersion turns out also to be a complex phenomenon, composed of a basic effect of photon retardation, which must originate in the periodic mass of the photons, superposed by another clearly distinct reaction (appearing in zones of absorption or resonance), due to their periodic reactivity. The equations: $(\lambda-X)(n-Y)=Q$, valid here, are of hyperbolic shape and point out that refraction is kinetically of the second order with respect to $1/\lambda$, and thus also indicate the periodical nature of photons.

This is also true for double refraction, the natural, as well as the effects of Kerr and Cotton-Mouton[2].

(5) Natural and electro-magnetic rotation of polarized light obey the same hyper-

bolic equations and can therefore be considered as reactions of the second order with respect to $1/\lambda$. In this case the effects seem to be exclusively due to the photon-mass, no sensitivity to resonance-absorption being detectable.

(6) For reflection available experimental data are rather imprecise. However, this phenomenon seems to be a function of $1/\lambda$ only indirectly, being complementary to some other reaction of photons, which itself can be expressed by the hyperbolic equation valid for refractions and rotations of polarised light.

These kinetic equations based on one-dimensional concentration of activity, proportional to $1/\lambda$, are surprisingly simple compared to any among the scores of formulas proposed until now for photon reactions. The calculations are straightforward, no fitting of coefficients being required. And the computed values fall easily within the limits of experimental errors, even for the case of refraction-dispersion, which has been subject to the most accurate measurements in optics. Such a simplicity of formulation and the validity of the same equations for all reactions may be considered as a further support for the above views on the periodic nature of photons.

Thus the wavelength of light appears as the fraction of its trajectory enclosing one cycle of photon-transformations from the state of energy into the state of mass. The happenings within these boundaries can be further characterized as follows: the lifetime of the active state in the photons must be independent of the wavelength; it has to be strictly the same throughout the entire spectrum, otherwise the above equations would not hold (possibly this lifetime is a fundamental constant ?). Also this lifespan must be rather short compared to the wavelength, to fulfil the requirements of Bouguire-Lambert-Beer's law about the proportionality between absorption and concentration.

II. Further Facts and Possibilities–FILMS OF SUB-λ THICKNESS.

The notion of periodical activity in photons which is nothing else than an offspring of Newton's "fits", of de Broglie's "wave-particles" and of Heisenberg's "uncertainty", is perfectly compatible with photon behaviour in general. The principle of Huygens, diffraction, interference, phase-jumps in reflection and refraction···and even the transparency of thin metallic films as well as their colors, which have remained an enigma since their discovery, can be easily understood on the basis of our assumption that interaction with photons occurs only at their periodically appearing active states. However, it seems highly interesting to strengthen our proofs by further experimentation.

The complexity of photon structure is indicated by experimental facts, like the polarization of light, or the production of both pairs of electrons and mesotrons. These being observable "fragments" of individual light-quanta, seem especially fit for the investigation of the periodical nature of photons. However, apparently there was nothing of this kind detected until now, probably because the experimental conditions were not set for the discrimination between the various states of the photons, the existence of which remained unsuspected.

An individual approach to single photons seems to be possible by the study of optical properties of films of sub-λ thickness. On the way through such layers periodically active photons ought to behave as follows: Only if the absorbing thickness (e) is equal or greater than $(\lambda' - L)$—λ' being the wavelength within the absorbent and L the fraction of λ' during which the photon is absorptive—will each of the incident photons find time to become active within the layer, whatever its phase when crossing the boundary. In layers of the thickness larger than $(\lambda' - L)$, by increasing the concentration of the absorbent, conditions ought to prevail as shown in figure 1: Whereas if (e) is smaller than $(\lambda' - L)$, only a part of the photons proportional to $e/(\lambda' - L)$ will attain the state of absorptivity, so that

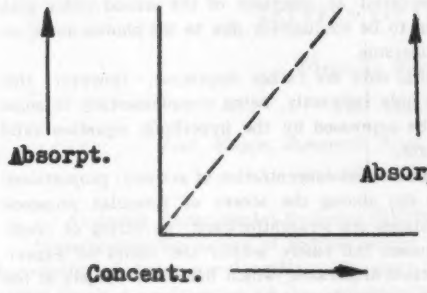

Fig. 1

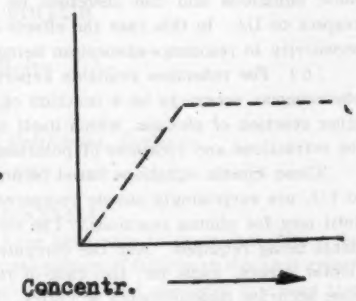

Fig. 2

whatever the concentration of the absorbent, capture shall never exceed a fraction of any incident intensity (Fig 2).

Qualitatively there is strong evidence for such screeding—Boyle in 1663 noticed the green color of gold films[3]. Later transparency of films to light has been studied on metals and a few other substances[4 through 25]. Striking optical properties have been discovered. Thin layers absorb proportionally less than massive ones. From the same sources it is also known that shifts of transparency occur towards greater wavelengths with increasing thickness of the layers. Recently Holden observed: light-yellow, orange-yellow, orange, purple, dark-purple, to be the transparency colors of siver layers of increasing thickness[26].

As yet these facts have not been explained satisfactorily. Electromagnetic theories had to be rejected[27,13,8]; ideas about the microstructure of thin layers, their increasing resistance to the movement of absorbing electrons, cannot be exact, since films in the state of superconductivity do not become more absorbent[6,9,11,14,15,17,28,29]. Faraday in 1857 has noticed the similarity of the colors of thin metallic films and the colloidal solutions of the same metals[31]. However ultramicroscopic and electron-microscopic studies show that the color of the films cannot be attributed to colloidal nature[8,17]. As late as 1950, it has been stated that no actual theory can explain the observed phenomena[16].

Figures 1 and 2 provide an explanation of the above facts. Furthermore it is almost certain that the optical properties of sub-λ films, if studied under the angle of periodicity in photons, will yield more information about individual light quanta: their evolution within periodical cycles, the length of the time (L) during which they are apt for absorption and scattering, phase relations of these two states, etc.

REFERENCES

(1) L. Akobjanoff: Photon Kinetics, [Berkeley 1955].
(2) L. Akobjanoff: unpublished data.
(3) F. Rosenberger: Geschichte der Physik [Braunschweig 1884] **2**, p. 159.
(4) A. T. Aschcheulov: Compt. Rend. Acad. Sci. [URRS] **24** (1939) 122.
(5) Th. Dreisch, Handbuch der Phvsik [Springer, Berlin 1929] **21**, p. 189 ff.
(6) T. Fukuroi, Sci. Pap. Inst. Phys. Chem. Res. [Tokyo] **32** (1937) 157.
(7) D. Hacman: Compt. Rend. **208** (1939) 1932.
(8) P. J. Haringhuizen et al: Physica **4** (1937) 695.
(9) R. Hilsch: Physik. Z. **40** (1939) 595.
(10) G. Jaffe: Handbuch der Experimental Physik [Leipzig 1928] **19**, p. 209 ff.

(11) K. Lauch: Ann. der Physik **74** (1924) 55.
(12) H. Ley: Handbuch der Physik [Springer, Berlin 1929] **21**, p. 20 ff.
(13) H. Murmann: Z. Physik. **80** (1933) 161.
(14) W. Planck: Physik. Z. **15** (1914) 563.
(15) B. Pogany: Ann. Physik. **49** (1916) 531.
(16) R. S. Sennet and G. D. Scott: J. Opt. Soc. Amer. **40** (1950) 203.
(17) R. A. Weale: Proc. Phys. Soc. [London] **62**B (1949) 576.
(18) H. Wolter: Z. Physik. **105** (1937) 269.
(19) R. W. Wood: Nature. **131** (1932) 582.
(20) C. Zener: Nature. **132** (1933) 968.
(21) M. Faraday: Trans. Roy. Soc. [London] **147** (1857) 145.
(22) J. Cayrel: Compt. Rend. **205** (1937) 488.
(23) M. Dorn and H. Name: Germ Pat. 690 973, Apr. 18, 1940.
(24) H. Mohler and P. Giger: Chimia. **1** (1947) 109.
(25) A. Pflueger: Wied. Ann. Physik and Chemie **65** (1898) 173, 225.
(26) J. Holden: Proc. Phys. Soc. [London] **62**B (1949) 405.
(27) P. Drude: Lehrbuch der Optik [Leipzig 1906].
(28) Falkenhagen: Handbuch der physikalischen Optik [Gehrke, Leipzig 1927] **1** p. 795.
(29) J. C. M. Garnett: Trans. Roy. Soc. [London] **203**A (1904) 385.